AUSTENITIZATION KINETICS

By

DEBAPRASAD DATTA

DEPARTMENT OF METALLURGICAL ENGINEERING

INDIAN INSTITUTE OF TECHNOLOGY KANPUR

JULY, 1979

AUSTENITIZATION KINETICS

A Thesis Submitted
In Partial Fulfilment of the Requirements
for the Degree of
MASTER OF TECHNOLOGY

By
DEBAPRASAD DATTA

to the

DEPARTMENT OF METALLURGICAL ENGINEERING
INDIAN INSTITUTE OF TECHNOLOGY KANPUR

JULY, 1979

CERTIFICATE

This is to certify that the thesis entitled "AUSTENITIZATION KINETICS" by Debaprasad Datta is record of work carried out under my supervision and has not been submitted elsewhere for a degree.

(A.M. GOKHALE)
Lecturer
Department of Metallurgical Engg.
Indian Institute of Technology, Kanpur

July, 1979

ACKNOWLEDGEMENTS

I take this opportunity to express my deep and profound sense of gratitude to Dr. A.M. Gokhale for suggesting this topic and for his constant guidance and encouragement throughout the course of this work.

I thank Mr. K.P. Mukherjee for his help in heat treatment and photography.

I also thank Mr. P. Sarkar and Mr. V.P. Gupta for helping in melting the alloy.

I thank all my friends without whom my stay here would not have been as enjoyable as it was.

Debaprasad Datta

ABSTRACT

Austenitization kinetics of Fe-0.15% C alloy has been studied at four different temperatures ranging from 800°C to 870°C. The initial microstructure was pearlite nodules distributed in the ferrite matrix. The transformation was monitored by estimating the volume fraction of austenite and the surface area of austenite - ferrite interface per unit volume by quantitative microscopy. It is concluded that the austenite growth geometry is two dimensional. Between 800°C to 840°C the radial growth of austenite can be described by a simple parabolic growth law. This indicates diffusion controlled growth of austenite in the temperature range of 800°C to 840°C.

CONTENTS

Page No.

LIST OF FIGURES

LIST OF TABLES

CHAPTER I

PROBLEM FORMULATION

Many phase transformations occur by the process of nucleation and growth. In such transformations, the nucleation rate and growth rate of the product phase are the two important kinetic variables. The global evolution of the microstructure during phase transformation depends on both the nucleation rate and growth rate. It follows that the global geometrical properties of the product phase (for example, volume fraction) are determined by nucleation rate and growth rate. However, the global geometrical properties are related to these kinetic variables in a very complex manner. The 'extended' or 'imaginary' volume fraction $V_{V_{ex}}(t)$ of the product phase and the 'extended' surface area of the product phase per unit volume $S_{V_{ex}}(t)$ are given by the following equations

$$V_{V_{ex}}(t) = K_V \int_0^t [R(t,\tau)]^3 \dot{N}(\tau)\, d\tau \qquad (1)$$

$$S_{V_{ex}}(t) = K_S \int_0^t [R(t,\tau)]^2 \dot{N}(\tau)\, d\tau \qquad (2)$$

where, $\dot{N}(\tau)$ is the nucleation rate of the product phase in 'extended' space at nucleation time τ and $R(t,\tau)$

is the 'extended' size of the product phase particle at process time t, whose nucleation time is τ. K_V and K_S are the shape factors. The geometrical impingement between the growing product phase particles is not taken into account in equations (1) and (2) and that is why the volume fraction and surface area calculated from the above equations are the 'extended' or 'imaginary' properties. The real volume fraction of the product phase V_V and the real surface area per unit volume S_V can be estimated from the corresponding 'extended' values by the use of impingement functions[1,2]. Alternatively, if the real volume fraction and surface area are measured at various times during isothermal transformation, the extended properties can be calculated (1,2). Thus, if $V_{V_{ex}}(t)$ and $S_{V_{ex}}(t)$ are known, equations (1) and (2) give two integral equations with two unknown functions, namely $\dot{N}(\tau)$ and $R(t,\tau)$. The function $R(t,\tau)$ is completely determined by the growth rate of the product phase. Hence, the solution of equations (1) and (2) can give the information about the nucleation rate and growth rate. However, equations (1) and (2) represent a system of simultaneous integral equations and the analytical solution cannot be obtained. The numerical techniques involve large processing errors and the resultant

information obtained on the nucleation rate and growth rate is almost meaningless. In order to make the problem mathematically tractable, usually some assumptions are made regarding the nucleation rate and growth rate[1]. It is then possible to obtain the quantitative information regarding nucleation rate and growth rate by utilizing equations (1) and (2). However, this approach has a serious draw back. The information obtained regarding the nucleation rate and growth rate depends critically on the assumptions made regarding these variables. Many times, this leads to a serious misinterpretation of the data.

The above drawbacks can be avoided if the nucleation rate variable can be completely eliminated by proper design of the experiments or by proper choice of the system. In such a case precise information regarding growth rate can be obtained from the time variation of the volume fraction and surface area of the product phase. The main aim of the present study is to explore the practical feasibility of such an approach. For this purpose, the austenitization kinetics of Fe-0.15% C alloy has been investigated.

At room temperature, the microstructure of slowly cooled Fe-0.15% C alloy consists of pearlite nodules distributed in the ferrite matrix. The austenitization process

of such a material occurs in two stages. In the first stage, pearlite transforms to austenite. At temperatures, higher than 800°C the pearlite to austenite transformation occurs in a less than one second.[3] At the end of the first stage, the microstructure consists of the austenite particles in the ferrite matrix. The number and size distribution of the austenite particles is identically equal to the number and size distribution of the pearlite nodules in the starting structure. The second stage of austenitization consists of the growth of austenite in the ferrite matrix. There is no further nucleation of austenite in the second stage. The total number of austenite particles (in the extended space) is the same as the number of pearlite nodules in the starting structure. Thus the nucleation rate variable is eliminated during the second stage of the austenitization process. The only important kinetic variable of the process is the austenite growth rate. The precise information regarding the austenite growth rate can be obtained from the time dependence of the global properties during an isothermal austenitization process.

In the present investigation, the volume fraction and surface area of austenite per unit volume, were measured at different times during austenitization of Fe-0.15% C alloy.

The experiments were performed at four different temperatures, ranging from 800°C to 870°C. The growth rate of austenite has been estimated from this data..

CHAPTER II

LITERATURE REVIEW

2.1 Introduction :

Austenitization kinetics of Fe-C alloys depends significantly on the starting microstructure. In the Fe-C alloys containing less than 0.2% carbon, the starting microstructures, usually encountered, are as follows :

(1) Pearlite nodules distributed in the ferrite matrix

(2) Spherodized cementite distributed in the ferrite matrix.

The kinetics of austenitization is quite different for the above two microstructures. In the first case, the austenitization process occurs in two stages. In the first stage, the pearlite nodules transform to austenite and the second stage consists of the growth of austenite in the ferrite matrix. In the case of second type of starting microstructure (i.e. spherodized cementite and ferrite aggregates) the austenite phase nucleates at the ferrite-spherodized cementite interface and grows by the diffusion of carbon from cementite to ferrite through the austenite layer. The diffusion geometry is different in the case of

the two starting microstructure and hence the kinetics of austenitization is also different.

Some experimental and theoretical work has been done on the austenitization kinetics of spherodized cementite and ferrite aggregates. However, not much work has been done on the austenitization of low carbon steel consisting of aggregates of ferrite and pearlite nodules.

2.2 Austenitization Kinetics of Spherodized Cementite and Ferrite Aggregates :

Roberts and Mehl[4] studied the austenitization kinetics of spherodized low carbon steel. They observed that the austenite forms around each carbide particle and grows into ferrite. Judd and Paxton[5] carried out a detailed quantitative investigation of the austenitization kinetics of a low carbon steel. They observed that spherodized cementite is situated on the grain edges of the ferrite matrix (which are the triple points on the plane of polish). Judd and Paxton[5] developed a theoretical model for the dissolution of spherodized cementite during the austenitization process. By assuming that the carbon diffusion through austenite is the rate controlling step and the carbon concentration profile can be approximated by that given by steady state condition, Judd and Paxton

derived the following equation for the dissolution of the spherodized cementite.

$$t = \frac{1}{2(D_c^{\gamma})_{r_b}} \left(\frac{C_1 - C_\alpha}{C_2 - C_1}\right) \left[r_o^2 (1+E) - r_b^2 - \frac{1}{E} \left(r_o^3(1+E) - r_b^3 E\right)^{2/3} \right] \quad \ldots\ (2.1)$$

where,

t = Process time

r_a = radius of cementite particle at time t

r_o = initial radius of cementite particle

r_b = outer radius of austenite shell

C = concentration of carbon in ferrite

C_2 = equilibrium carbon concentration at the $Fe_3C - \gamma$ interface

C_1 = equilibrium carbon concentration at the $\gamma - \alpha$ interface

C_c = concentration of carbon in cementite

$$E = \frac{(D_c^{\gamma})_{r_a}}{(D_c^{\gamma})_{r_b}} \left[\frac{C_1 - C_\alpha}{C_c - C_2} \right]$$

$(D_c^{\gamma})_{r_a}$ = diffusion coefficient of carbon in austenite near $Fe_3C - \gamma$ interface

$(D_c^{\gamma})_{r_b}$ = diffusion coefficient of carbon in austenite near $\gamma - \alpha$ interface

Judd and Paxton[5] monitored the spherodized cementite particle size by quantitative microscopic techniques. A good agreement was observed between the experimentally determined growth path of spherodized cementite and that predicted by equation (2.1).

Speich and Szirmae[6] observed that the austenite nucleates at the triple lines between cementite and ferrite grain boundaries. They also concluded that the austenitization kinetics is controlled by the rate of diffusion of carbon through austenite. Niedzwiedz, Weiss and Partom[7] have developed a more sophisticated model for the dissolution of spherodized cementite during austenitization. Their treatment involves a numerical solution to a nonlinear partial differential equation with two floating boundary condition.

2.3 Austenitization Kinetics of Pearlite Nodules and Ferrite Aggregates :

Karlson[8] has studied the transformation kinetics of the austenitization process in Fe-0.18% C alloy at 855°C. The transformation was monitored by estimating the volume fraction of austenite at different times during the isothermal austenitization process at 855°C. The pearlite transforms to austenite in less than one second and the further transformation takes place by consumption of ferrite by the

existing austenite grains. Karlson[8] has developed a theoretical model for the second stage of the austenitization process (i.e. growth of austenite into ferrite matrix). He assumed that the austenite particles have a spherical shape and the rate controlling mechanism is the diffusion of carbon in austenite. In order to estimate the growth rate of austenite, it is necessary to get a solution to the Fick's second law in the spherical co-ordinates with a moving boundary condition. Since a closed form solution can not be obtained and the numerical solution is too complicated, Karlson made the following approximation to solve the problem[6]. A closed form analytical solution is available for the decarburization of a sphere[9]. Karlson, extrapolated the concentration profile obtained from such a solution beyond the sphere radius. The concentration of carbon was plotted as a function of distance for different process times. The radial co-ordinate at which the concentration of carbon was equal to conc. of carbon in austenite in equilibrium with ferrite (obtained from phase diagram) was assumed to give the position of $\gamma - \alpha$ interface (i.e. radius of austenite particle). In this manner, the radius of austenite particle was calculated as a function of time. Karlson[8] further assumed that all the austenite particles are of same size. With these assumptions, he

calculated the volume fraction of austenite as a function of time. These calculated values of volume fraction were compared with the experimentally estimated values of volume fraction of austenite at various time. The agreement between the theoretical and experimental values was poor (particularly at large volume fractions). The poor agreement between the experimental and theoretical behaviour is probably due to the following reasons.

(1) Karlson completely neglected the geometrical impingement between growing austenite particles for the calculation of volume fraction from the theoretical model. The impingement correction is expected to be very important at large volume fractions.

(2) Extrapolation of the concentration profile for the decarburization of sphere beyond the fixed sphere radius has no physical meaning.

(3) Assumption of the three dimensional spherical growth geometry is not applicable to the austenite growth (this will be rigorously demonstrated in Chapter 5).

Karlson's data was reanalyzed during the present investigation. A plot of $V_V/1-V_V$ vs. t (where, V_V is the volume fraction of austenite) was found to be linear. This plot is shown in figure - 1. This experimental behaviour can be explained by the model developed in Chapter 5.

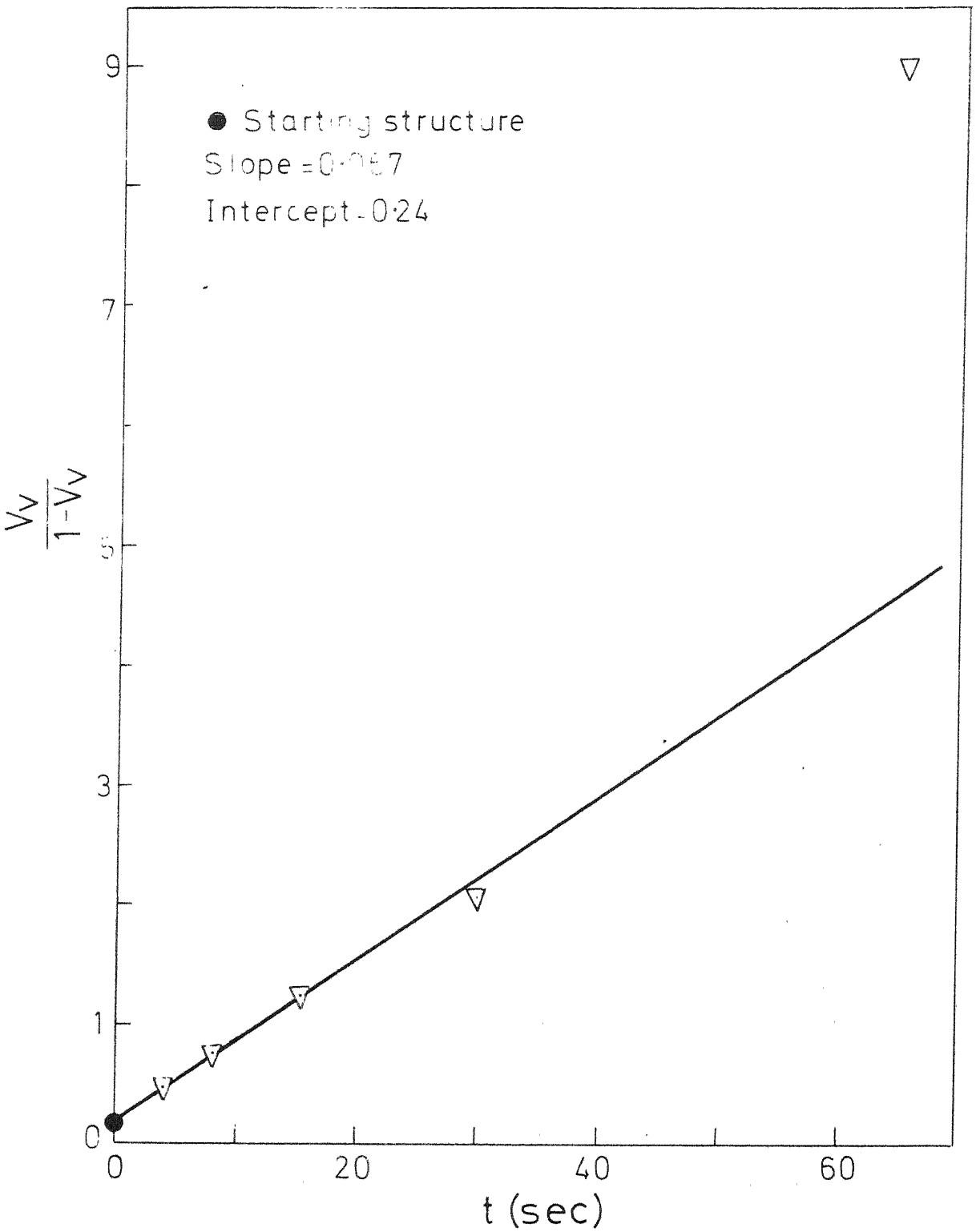

Fig.1 Plot of $\frac{V_V}{1-V_V}$ Vs t at 855°C as obtained from Kartson's data

CHAPTER III

QUANTITATIVE MICROSCOPIC TECHNIQUES

A description of quantitative microscopic techniques used in the present experimental work and the subsequent data analysis is given in this chapter.

3.1 Estimation of Volume Fraction :

In 1848 Delesse[9] showed that the average value or the 'expected' value of the area fraction $\bar{A}_A$ occupied by the phase of interest in the plane of polish is equal to its volume fraction V_V in the microstructure.

$$V_V = \bar{A}_A \qquad (3.1)$$

The above equation is statistically exact. No assumption or knowledge regarding particle shape and size is necessary for the estimation of volume fraction. However, the area fraction must be measured on the representative microsections. This method of estimation of volume fraction is called 'areal' analysis. It is a very tedious method if the measurements are performed manually.

Rosiwal[10] showed that if a test line is placed on the plane of polish, then the average value of the

fraction of test line length $\bar{L}_L$ contained in a particular phase is equal its volume fraction

$$V_V = \bar{L}_L \qquad (3.2)$$

It is not necessary to randomize the test line with respect to its angular spatial orientation. The relationship is statistically exact and it is valid for any shape and size. This method of estimation of volume fraction is called the 'lineal' analysis.

The volume fraction can be also estimated by 'point counting' method. This simple technique was developed by Thomson[11] and Glagolev[12]. If a number of test points are placed on the plane of polish, then the average value of the fraction of test points $\bar{P}_p$ contained in a particular phase is equal to its volume fraction.

$$V_V = \bar{P}_p \qquad (3.3)$$

Equation (3.3) is valid for a non random array of test points (e.g. intersections of a square lattice) provided the grid is placed at random on a representative microsection. If a grid of test points is used for point

counting, then it is called 'systematic point counting'. The equation (3.3) is also statistically exact and valid for any type of homogenous (i.e. no segregation) microstructure. It has been shown that systematic point counting involves less effort than areal analysis or lineal for a given accuracy[13]. In the present work, the volume fraction of austentile was estimated manually by point counting. A square grid was inserted in the eye piece of the microscope for this purpose.

3.2 Estimation of Surface Area Per Unit Volume :

The surface area per unit volume S_V, of any type of interface present in the microstructure, can be unambiguously estimated from the measurements made on a representative two dimensional section through the three dimensional microstructure. Suppose, a test line is placed at random on the plane of polish. Let N_L be the number of intersections of this test line with the traces of the interface of interest in the plane of polish per unit test line length. Suppose the experiment is repeated with the various orientations of the test line and various frames of observation. Let $\bar{N}_L$ be the average value of N_L obtained from all these measurements. It can be shown that the surface area per unit volume S_V of the interface of interest

is related to the corresponding value of $\bar{N}_L$ by the following equation

$$S_V = 2 \bar{N}_L \qquad (3.4)$$

This equation was derived independently by Saltykov[14] and Smith and Guttman[15]. It is a statistically exact equation and it is valid for interface elements of any arbitrary curvature. Thus no assumption or knowledge regarding shape or size is necessary for the estimation of S_V. This method for estimation of S_V is called the 'line intercept counting'. If the microstructure is isotropic (i.e. no preferred orientation) and homogenous (i.e. no segregation), then a single test line orientation can give a reliable estimate of S_V. However, measurements on a large number of frames of observation (different locations on the plane of polish) are necessary to get a reliable estimate of $\bar{N}_L$ and hence S_V. The statistical error involved in the estimation of S_V can be kept as small as desired by increasing the number of measurements. In the present investigation the surface area of γ-γ interface per unit volume was estimated manually by performing measurements directly under the microscope. A square grid was inserted in the eye piece of the microscope for this purpose.

3.3 Concept of Extended Structure and Impingement Correction Factors :

Imagine a structure calculated from some model based on assumed nucleation rate and growth rate. If the standard method for calculating the volume fraction and surface area of the product phase are used then such calculations over estimate the values of the geometrical properties. The magnitude of this over estimation increases with the increasing volume fraction of the product phase. The over estimates result because the theoretical models for nucleation rate or growth rate ignore the geometrical impingement between the growing product phase particles. Thus the theoretical models allow the product phase particles to grow into one another. This obviously can not happen. The microstructure calculated from theoretical model is called 'extended' or 'imaginary' microstructure and the volume fraction and surface area calculated from such models are'extended' volume fraction $V_{V_{ex}}$ and the 'extended' surface area $S_{V_{ex}}$. These extended geometrical properties monotonically increase with time and they approach infinity as $t \rightarrow \infty$. However, it is possible to estimate the real volume fraction of the product phase V_V and the real surface area S_V if the corresponding extended values are known.

Jhonson and Mehl[16] have shown that if the particle centres are <u>randomly</u> distributed then,

$$V_V = 1 - \text{Exp}\left(- V_{V_{ex}} \right) \qquad (3.5)$$

and

$$S_V = (1-V_V).\ S_{V_{ex}} \qquad (3.6)$$

Dehoff[17] has shown that if the particles centres are 'clustered' instead of randomly distributed then,

$$\frac{V_V}{1 - V_V} = V_{V_{ex}} \qquad (3.7)$$

and

$$S_V = (1 - V_V)^2\ S_{V_{ex}} \qquad (3.8)$$

Thus it is possible to convert the real fraction and surface area to their corresponding extended values and vice versa for the purpose of data analysis.

CHAPTER IV

EXPERIMENTAL WORK

The austenitization kinetics of Fe-0.15% C alloy was studied at 800°C, 820°C, 840°C and 870°C.

4.1 Materials :

The Fe-C alloy was prepared from 99.99% pure Fe and high purity graphite. An alloy of nominal composition Fe-0.15% C was made by melting appropriate amounts of Fe and C in an induction furnace in the argon atmosphere. The alloy was melted twice in order to ensure the chemical homogenity. The alloy was kept in the liquid state for about five minutes for liquid state homogenization and then it was allowed to cool slowly in the induction furnace. The alloy button was hot forged at approximately 1100°C. A layer of 1/16" thickness was removed from all the external surfaces of the not forged sample by machining. This was done to remove the decarburized layer. The alloy was then cold swaged to get a rod of 0.3" diameter. The samples of approximately 1/8" thickness were cut from the cold swaged rod of 0.3" diameter. Approximately, fortyfive samples of 1/8" thickness and 0.3" diameter were obtained. Three randomly selected samples were prepared for microscopic

examination. The microstructure of these samples contained elongated Pearlite patches in the ferrite matrix. The microstructure was similar in all the samples and it was uniform in each sample. The volume fraction of pearlite was approximately same in all the samples. The seggregation was virtually absent.

4.2 Preliminary Heat Treatment :

This heat treatment was carried out to produce the starting microstructure for the austenitization kinetics studies. The samples were vacuum sealed in Vycor tubes. The vacuum sealed samples were kept in a furnace at 900°C for one hour. The power to the furnace was then cut off and the samples were allowed to cool in the furnace. This treatment produced uniformly distributed equiaxed patches of pearlite in the ferrite matrix.A representative microstructure is shown in Figure-2. It is interesting to note that most of the pearlite nodules are situated on the grain edges of the ferrite matrix (which appear as triple points on the plane of polish). The volume fraction ~~was~~ of pearlite was estimated by point counting method. The measurements were made on twenty different frames of observation. The volume fraction of pearlite was found to be equal to 0.16. The surface area of Pearlite-ferrite interface per unit volume

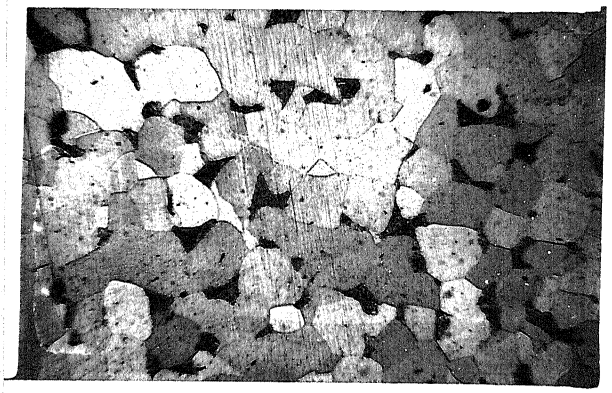

FIG. 2. A representative starting microstructure (Magnification : 150 X)

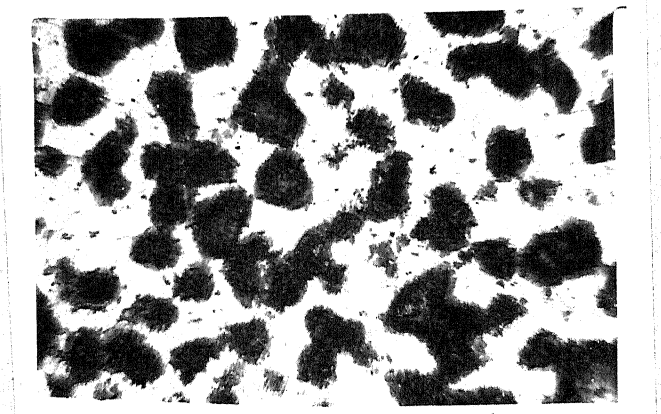

FIG. 3. A partially transformed microstructure after heating at 870°C for 20 sec. (Magnification : 150 X)

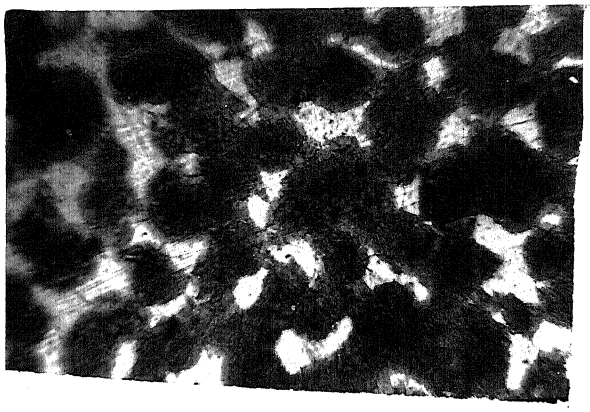

FIG. 4. A partially transformed microstructure after heating at 870°C for 40 secs. (Magnification : 150 X).

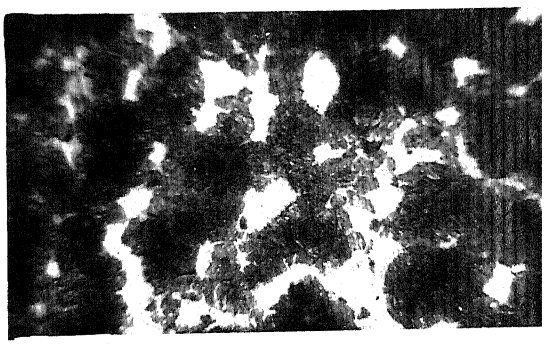

FIG. 5. A partially transformed microstructure after heating at 870°C for 60 sec. (Magnification : 150 X)

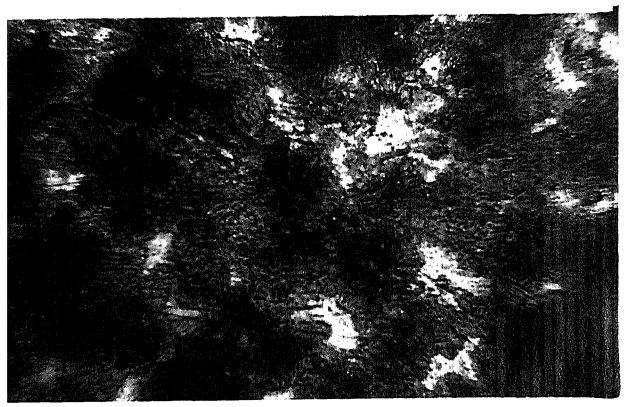

FIG. 6. A partially transformed microstructure after heating at 870°C for 80 secs. (Magnification : 150 X).

was estimated by performing the line intercept counting on twenty different frames of observation. The surface area was found to 218 cm^2/cm^3.

4.3 Austenitization Experiments :

In order to monitor the austenitization kinetics it is necessary to produce a series of partially transformed samples at various austenitization temperatures. This was done as follows.

The samples were kept in a lead bath maintained at 870°C for various times ranging from 15 sec. to 80 sec. and then they were quickly quenched in water. The procedure was repeated at 800°C, 820°C and 840°C. At 800°C the samples were kept in the lead bath for various times ranging from 30 sec. to 240 sec., where as at 820°C and 840°C the reaction times ranged from 30 sec. to 180 sec. and 20 sec. to 120 sec. respectively. The water quenching of the partially transformed samples produced microstructures consisting of ferrite and martensite (which was austenite at the reaction temperatures).

4.4 Metallography :

The surface layer of the flat faces of all the samples was removed by filing. The samples were then mounted in bakelite. The polishing was carried out by

using standard polishing technique. In order to obtain a good contrast between ferrite and martensite, a solution of sodium meta bi-sulphite was used as an etching agent. The composition of etching agent and other details are given in Table - 1. The microstructures were observed at 200 X. The representative microstructures of some samples reacted at 870°C are shown in figures 3 to 6. In these micrographs, dark phase is martensite (which was austenite at the reaction temperature) and bright phase is ferrite.

4.5 Quantitative Microscopy :

The volume fraction of austenite (martensite in the quenched samples) and surface area of austenite - ferrite interface per unit volume were estimated by quantitative microscopic methods (the details of these techniques are given in Chapter III). These measurements were performed on each partially transformed sample. A square grid was inserted in the eye piece of the microscope and the quantitative measurements were carried out directly under microscope. All measurements were carried out at 200 X. The same objective and eyepiece was used for all the measurements. The volume fraction was estimated by the point counting method and the surface area was estimated by the intercept counting. In order to get the reliable estimates of the

TABLE 1

Etching reagent used for the microscopic examination of ferrite-matensite structure :

Sodium meta bisulphite	Water	Etching temperature	Etching time
20 gm	100 ml.	Room temperature	45 Sec.

stereological parameters, in each sample the measurements were performed on atleast twenty different frames of observation. The values of volume fraction of austenite and surface area of austenite - ferrite interface per unit volume at various reaction times and temperatures are given in the tables 2 to 5.

TABLE 2

The volume fraction of austenite and the surface area of ferrite-austenite interface per unit volume at 800°C :

Time (Sec.)	Volume fraction of austenite, V_V	Surface area of ferrite-austenite interface per unit volume, S_V (cm^2/ cm^3)
0	0.16	218.00
30	0.206	240.50
60	0.259	270.00
90	0.296	295.75
120	0.315	306.00
150	0.333	325.00
180	0.355	329.52
210	0.378	335.00
240	0.39	339.62

TABLE 3

The volume fraction of austenite and the surface are of ferrite-austenite interface per unit volume at 820°C :

Time (sec.)	Volume fraction of austenite, V_V	Surface area of ferrite-austenite interface per unit volume, $S_V(cm^2/cm^3)$
0	0.16	218.00
30	0.231	249.50
60	0.296	312.00
90	0.342	335.70
120	0.377	346.00
150	0.420	370.00
180	0.450	365.62

TABLE 4

The volume fraction of austenite and the surface area of ferrite-austenite interface per unit volume at 840°C :

Time (sec.)	Volume fraction of austenite, V_V	Surface area of ferrite-austenite interface per unit volume, $S_V(cm^2/cm^3)$
0	0.16	218.00
20	0.331	301.00
40	0.444	365.45
60	0.523	374.00
80	0.579	345.62
100	0.629	338.00
120	0.661	310.65

TABLE 5

The volume fraction of austenite and the surface area of ferrite-austenite interface per unit volume at 870°C :

Time (Sec.)	Volume fraction of austenite, V_V	Surface area of ferrite austenite interface per unit volume, $S_V (cm^2/cm^3)$
0	0.16	218.00
15	0.35	350.00
20	0.41	361.50
25	0.49	390.00
30	0.56	360.00
35	0.62	352.81
40	0.672	305.00
50	0.75	260.70
60	0.81	200.00
70	0.868	151.67
80	0.94	52.00

CHAPTER V

RESULTS AND INTERPRETATIONS

5.1 Relationship Between S_V and V_V :

A plot of surface area of the austenite-ferrite interface per unit volume S_V vs. the volume fraction of austenite V_V is shown in figure-7. It is observed that the data points at <u>all</u> the austenitizing temperatures and times fall on a single curve. This indicates that the relationship between S_V and V_V is <u>independent</u> of temperature and it depends only on the initial structure. The plot appears to be parabolic and the maximum occurs at a value of V_V approximately equal to 0.5. This indicates a parabolic relationship of the type;

$$S_V = K\, V_V\, (1-V_V) \qquad (5.1)$$

where, K should be independent of austenitization temperature.

If the above relationship holds, then a plot of $S_V/(1-V_V)^2$ vs. $V_V/(1-V_V)$ should be linear at all the temperatures and the slope should be equal to K in equation (5.1). The plots of $S_V/(1-V_V)^2$ vs. $V_V/(1-V_V)$ at various temperatures are shown in figures 8 to 11. The slopes of these plots are given in Table- 6.

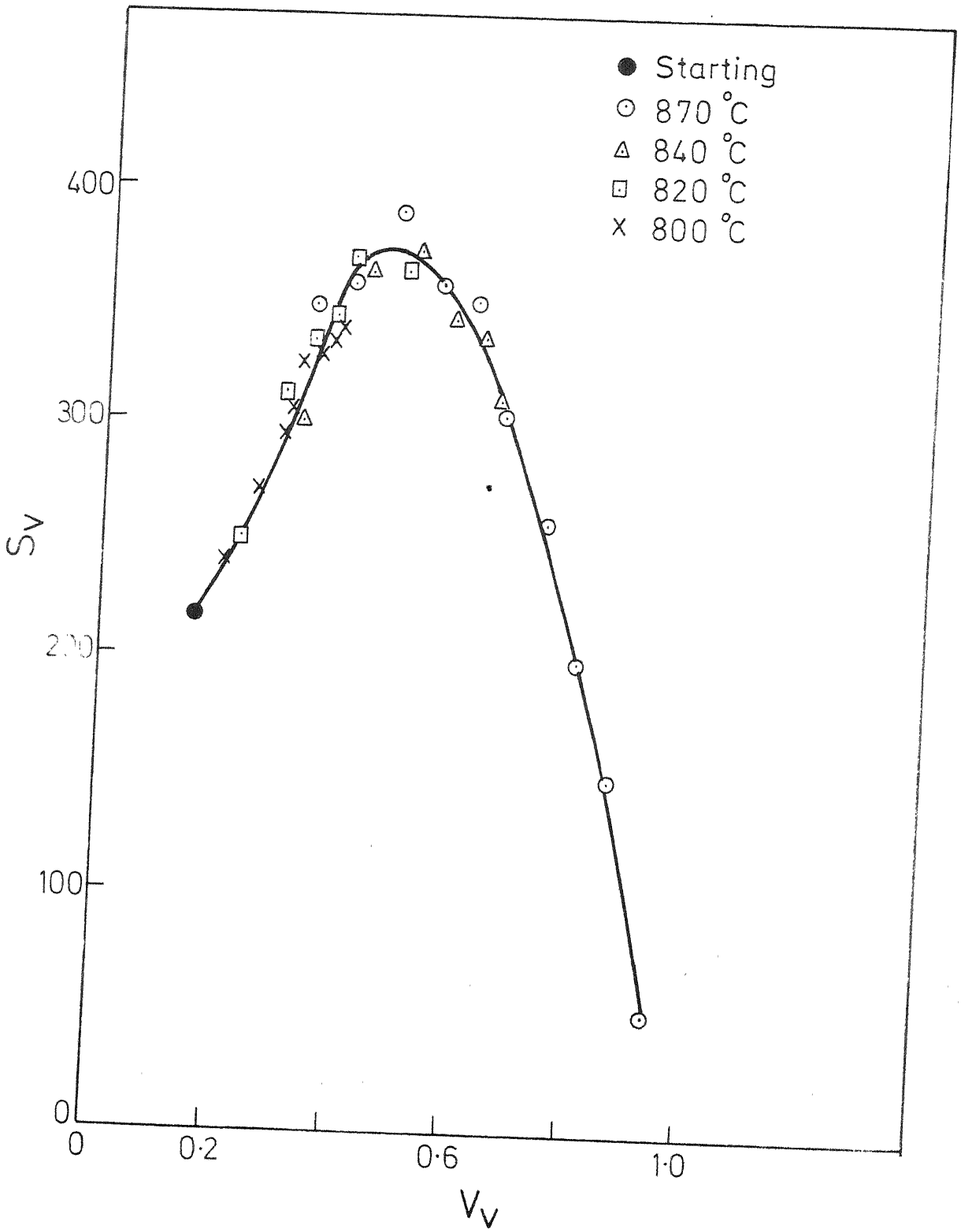

Fig.7 Plot of S_V Vs V_V

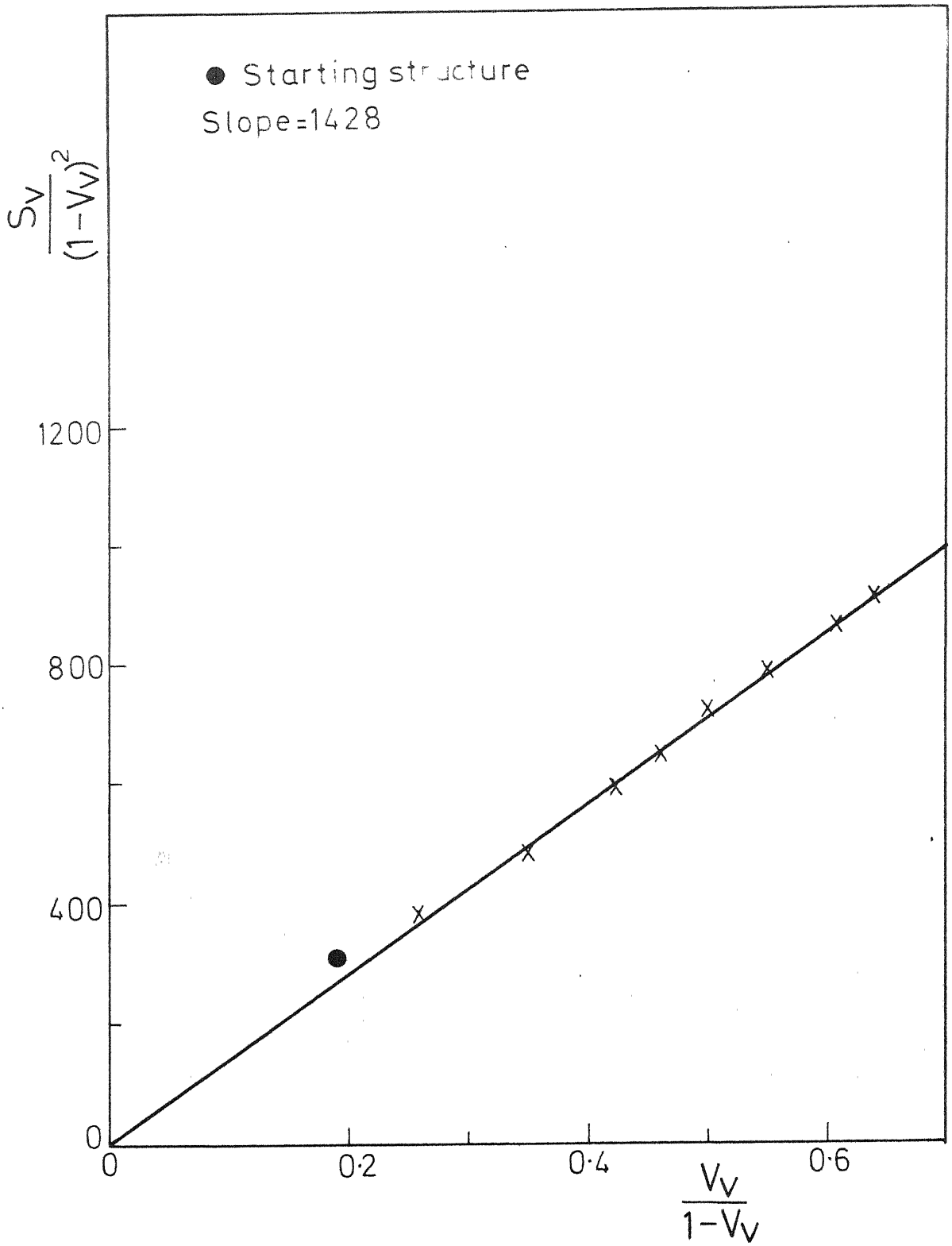

Fig.8 Plot of $\frac{S_V}{(1-V_V)^2}$ Vs $\frac{V_V}{1-V_V}$ at 800 °C

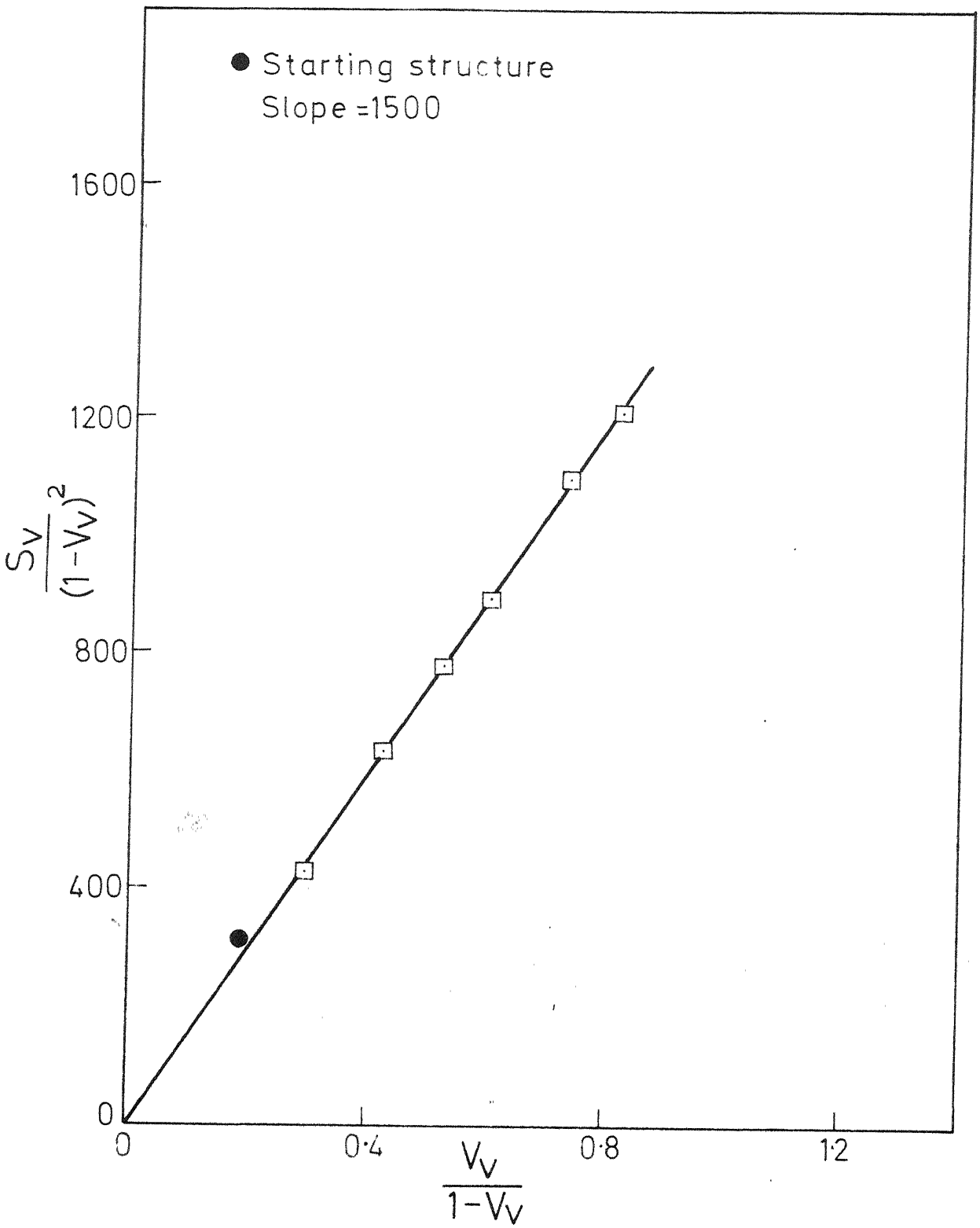

Fig. 9 Plot of $\frac{S_V}{(1-V_V)^2}$ Vs $\frac{V_V}{1-V_V}$ at 820 °C

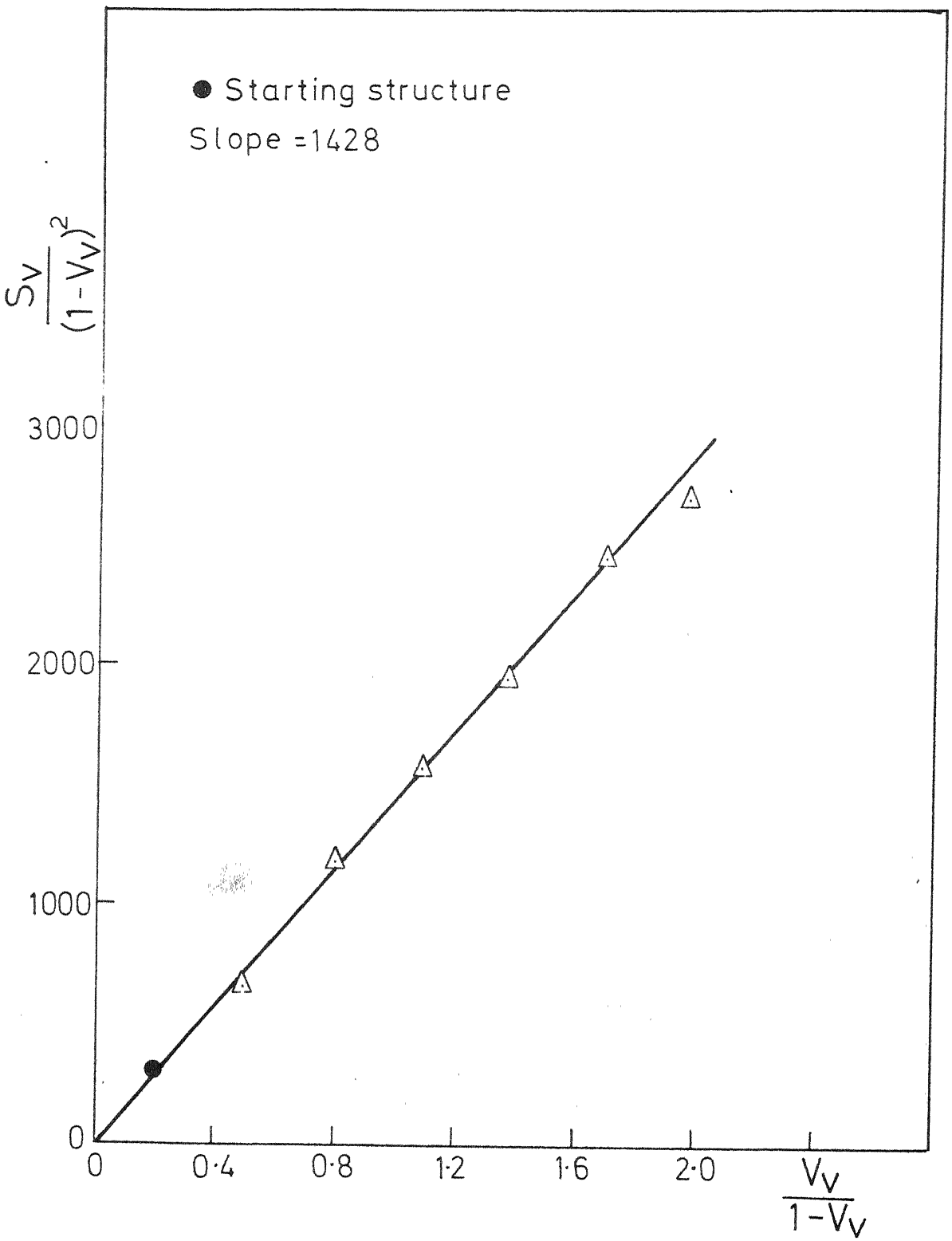

Fig.10 Plot of $\frac{S_V}{(1-V_V)^2}$ Vs $\frac{V_V}{1-V_V}$ at 840 °C

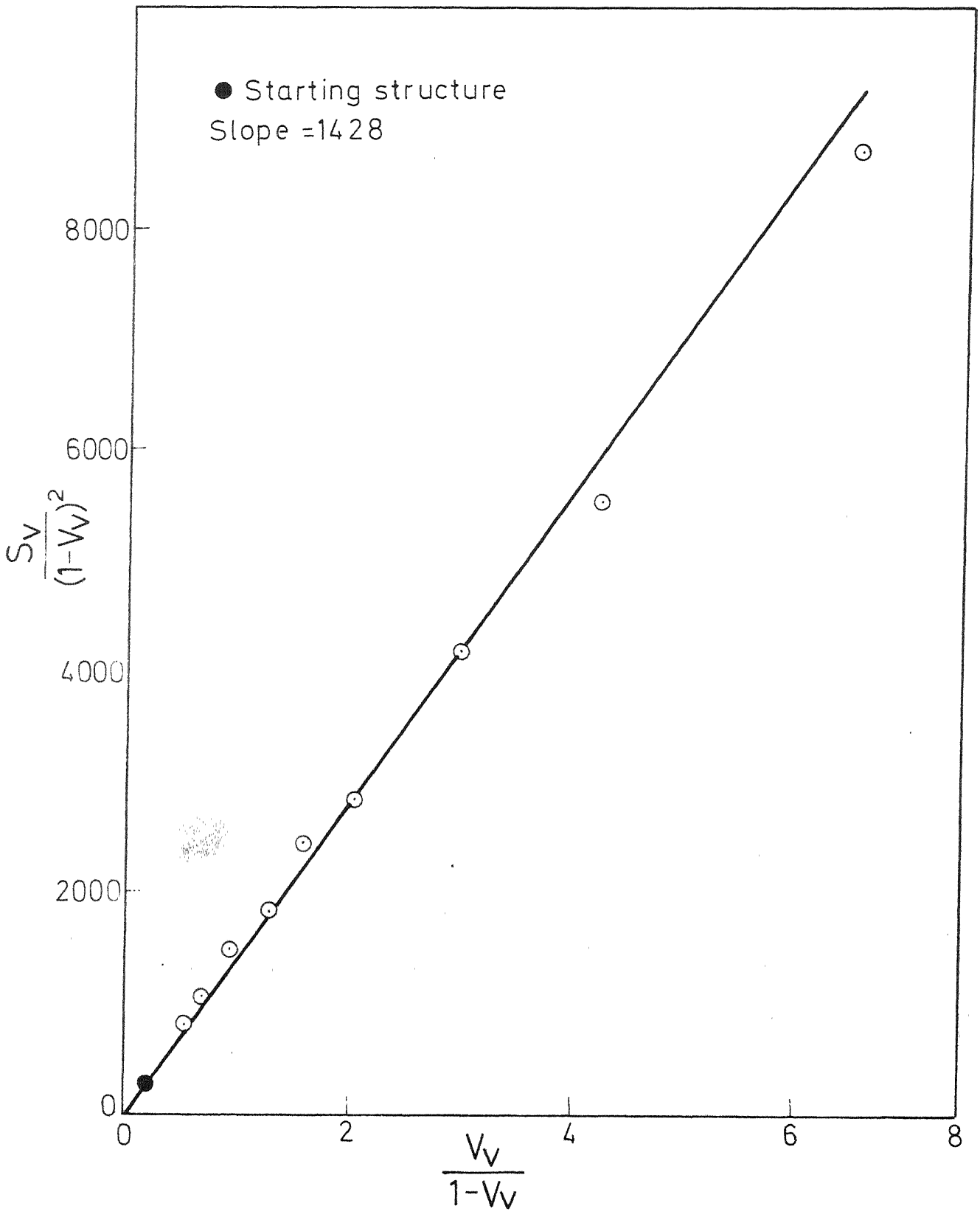

Fig.11 Plot of $\frac{S_V}{(1-V_V)^2}$ Vs $\frac{V_V}{1-V_V}$ at 870 °C

TABLE 6

T°C	Slope = K cm^2/cm^3
800	1428
820	1500
840	1428
870	1428

The slope of $S_V/(1-V_V)^2$ vs. $V_V/(1-V_V)$ is thus independent of temperature and all the plots pass through the origin. Thus,

$$\frac{S_V}{(1-V_V)^2} = \frac{K\ V_V}{(1-V_V)} \qquad (5.2)$$

or $$S_V = K\ V_V\ (1-V_V) \qquad (5.3)$$

where, K = 1446 cm^2/cm^3. This value of K is the average value obtained from Table 6. Thus the relationship between S_V and V_V is described by equation (5.3) for <u>all</u> the austenitizing temperatures and times.

5.2 Time Dependence of the Austenite Volume Fraction :

A plot of $V_V/(1-V_V)$ vs. t (where V_V is the volume fraction of austenite at process time t) is shown in figures 12 to 15 for the various austenitizing temperatures. It is observed that $V_V/(1-V_V)$ varies linearly with the process time t at 800°C, 820°C and 840°C. However, the plot of $V_V/(1-V_V)$ vs. t is non linear at 870°C (figure-15). Thus between 800°C to 840°C, the time dependence of austenite fraction can be described by the following equation.

$$\frac{V_V}{1-V_V} = 0.19 + Bt \qquad (5.4)$$

The, parameter B is the slope of $V_V/(1-V_V)$ vs. t straight line. The values of B at 800°C, 820°C and 840°C are given in Table-7.

TABLE - 7

T°C	B per sec.
800	0.00166
820	0.00362
840	0.015

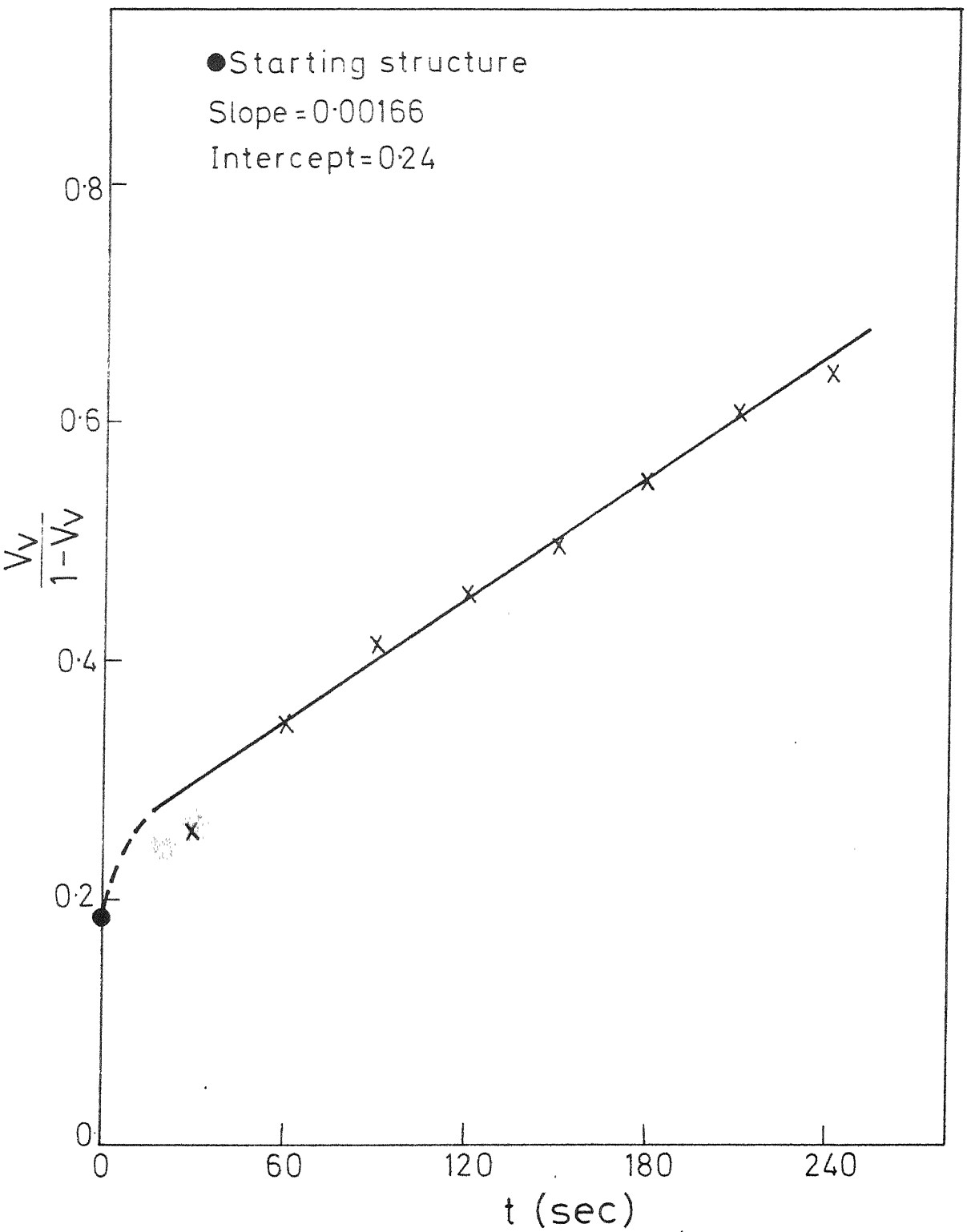

Fig.12 Plot of $\frac{V_V}{1-V_V}$ Vs t at 800 °C

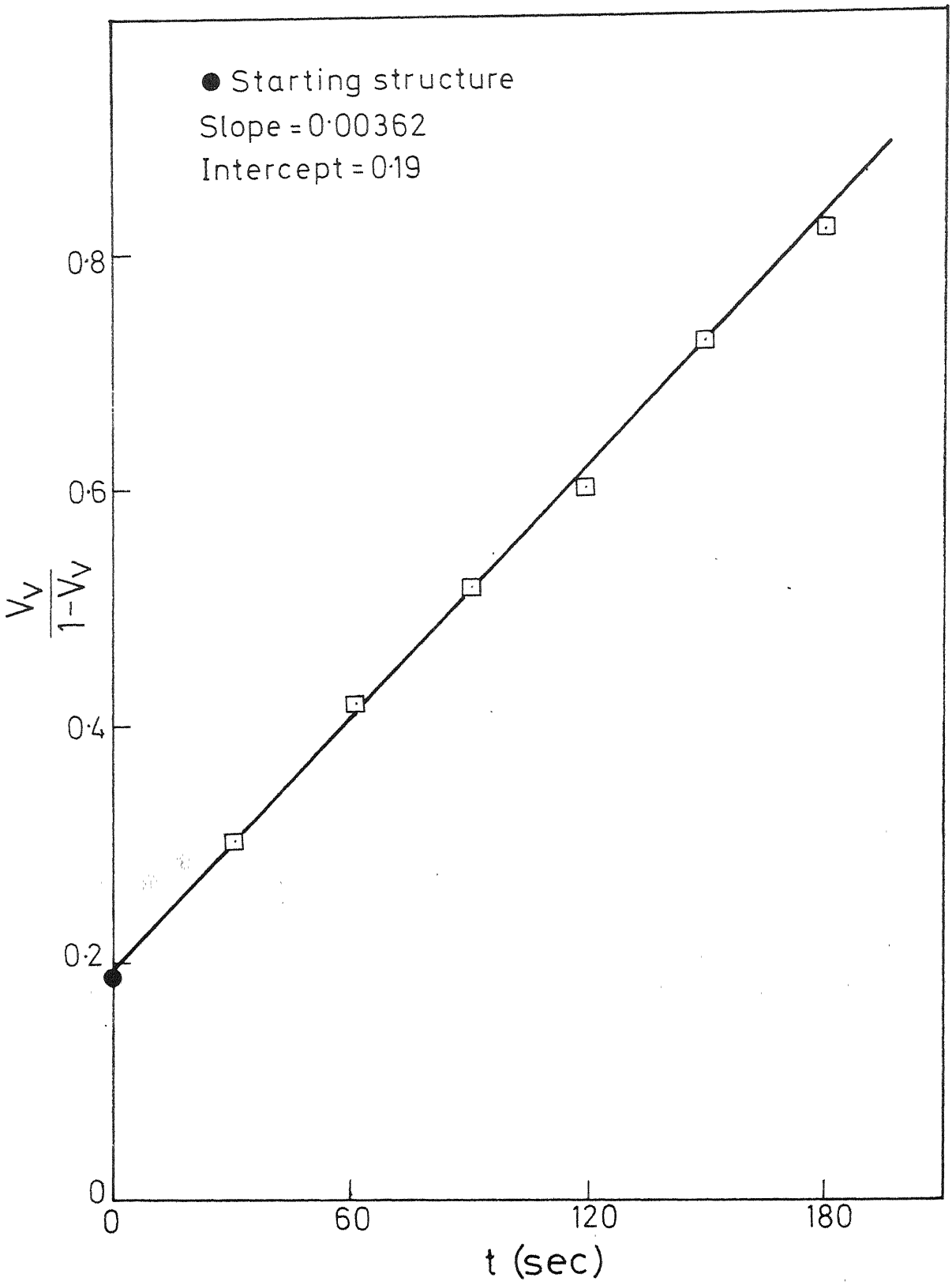

Fig.13 Plot of $\frac{V_V}{1-V_V}$ Vs t at 820 °C

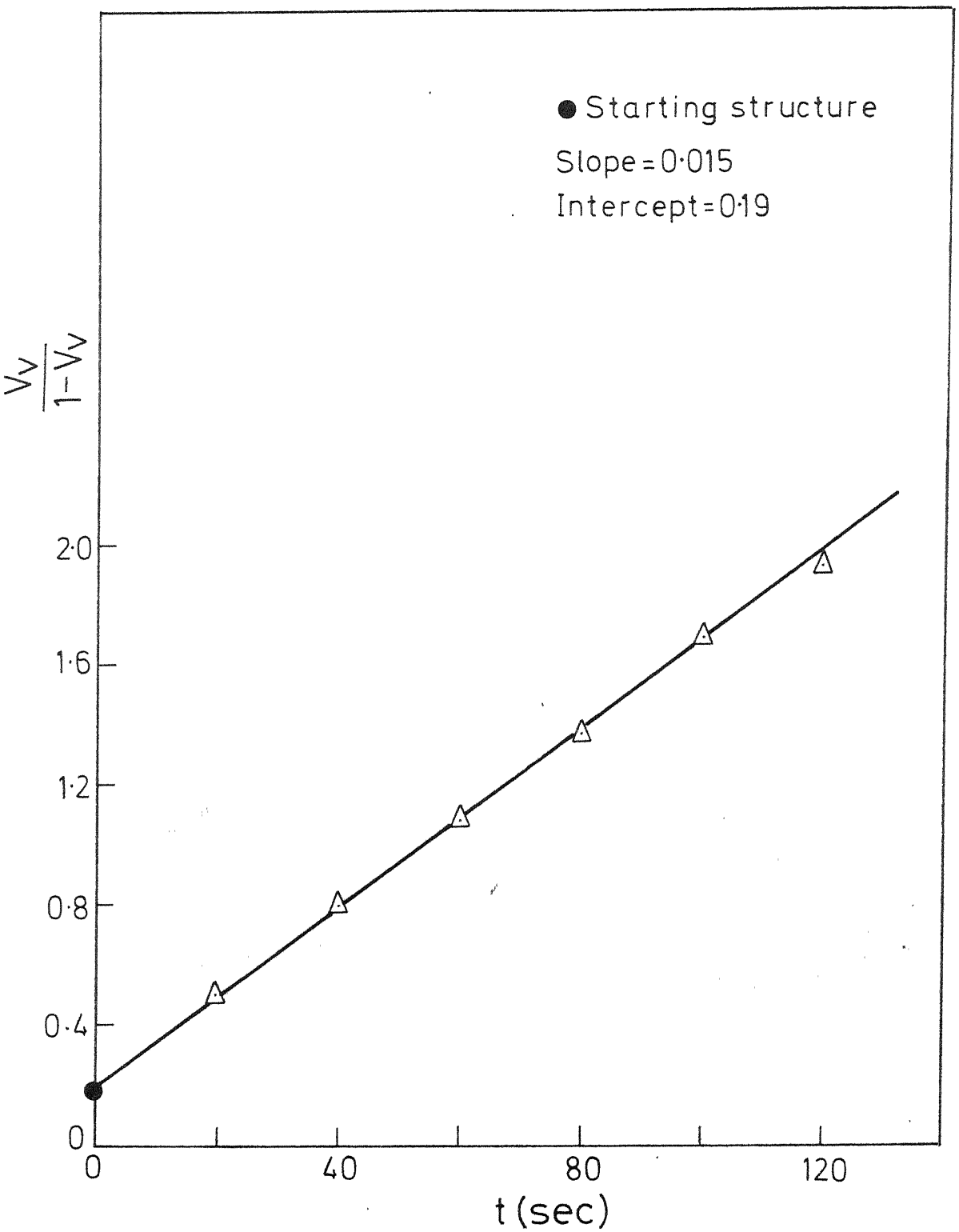

Fig.14 Plot of $\frac{V_V}{1-V_V}$ Vs t at 840 °C

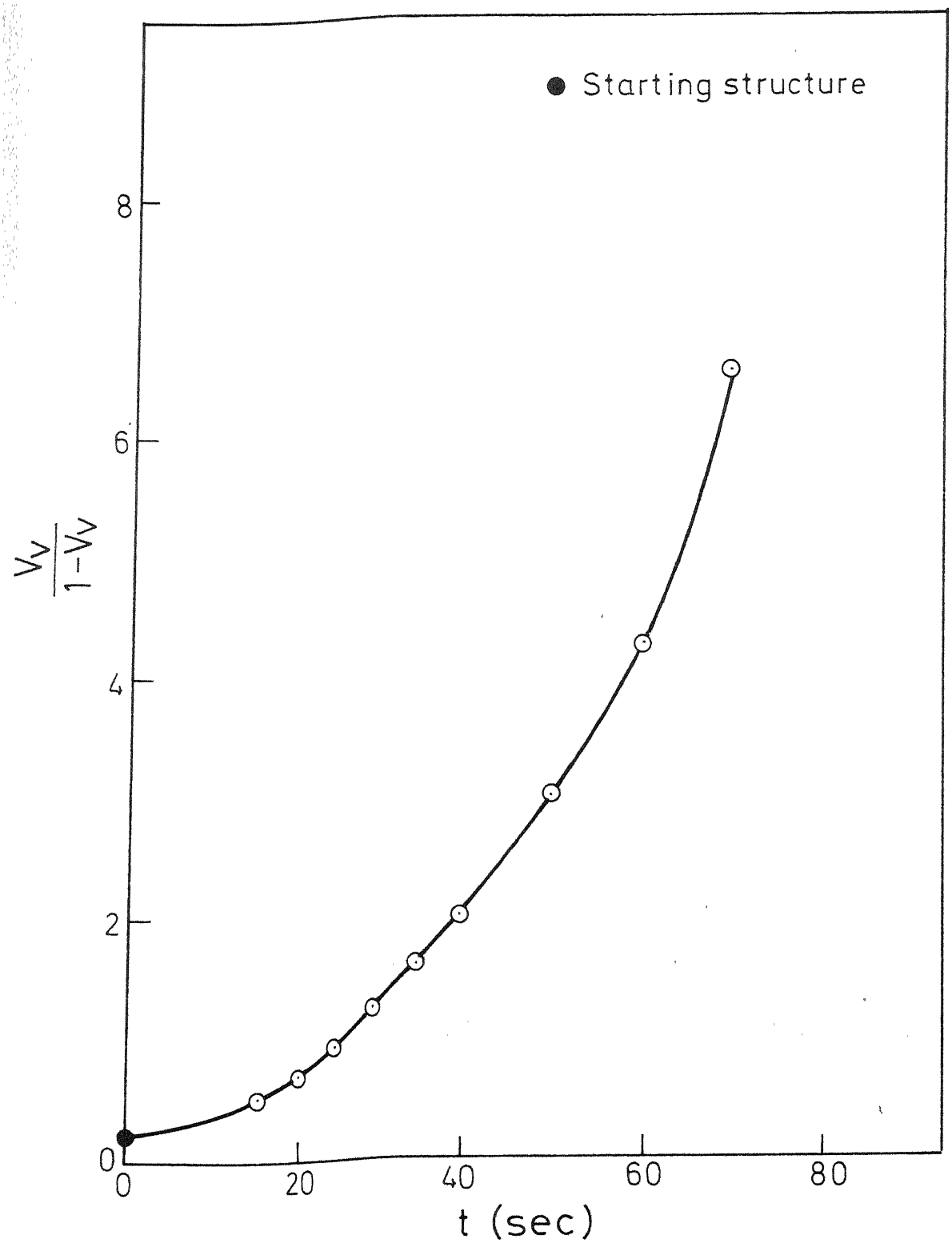

Fig.15 Plot of $\frac{V_V}{1-V_V}$ Vs t at 870°C

Thus the parameter B is a function of austenitizing temperature. The plot of $V_V/(1-V_V)$ vs. t at 870°C (figure-15) is non linear. This indicates that the kinetics of the process at 870°C is different from that between 800° and 840°C. It is interesting to note that a plot of $V_V/(1-V_V)$ vs. t for the Karlson's data[8] on the austenitization kinetics of Fe-0.18%C alloy at 855°C is also linear (see figure-1). A plot of $V_V/(1-V_V)$ vs. t^2 at 870°C is shown in figure-16. Thus at 870°C, the time dependence of volume fraction can be described by the following equation.

$$\frac{V_V}{1-V_V} = B_1 t^2 + 0.19 \qquad (5.5)$$

where, $B_1 = 0.00113$ per sec^2.

5.3 Time Dependence of Austenite-Ferrite Interfacial Area per Unit Volume :

A plot of $S_V/(1-V_V)^2$ vs. t at various austenitizing temperatures is shown in the figures 17 to 20. It is observed that at 800°, 820° and 840°C, the plot is linear. Thus, the time dependence of S_V between 800° and 840°C can be described by the following equation.

$$\frac{S_V}{(1-V_V)^2} = 308 + Et \qquad (5.6)$$

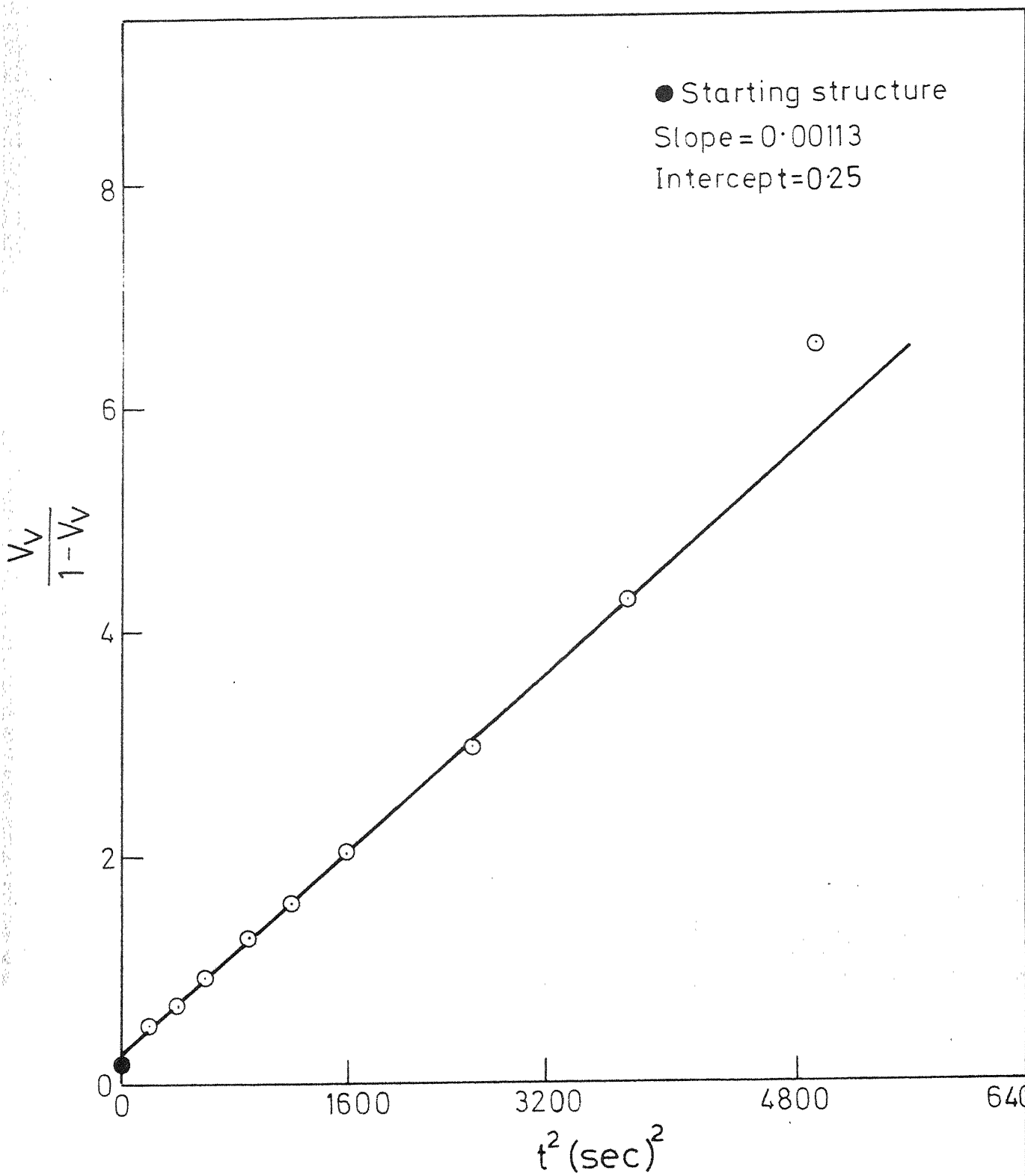

Fig.16 Plot of $\frac{V_V}{1-V_V}$ Vs t^2 at 870 °C

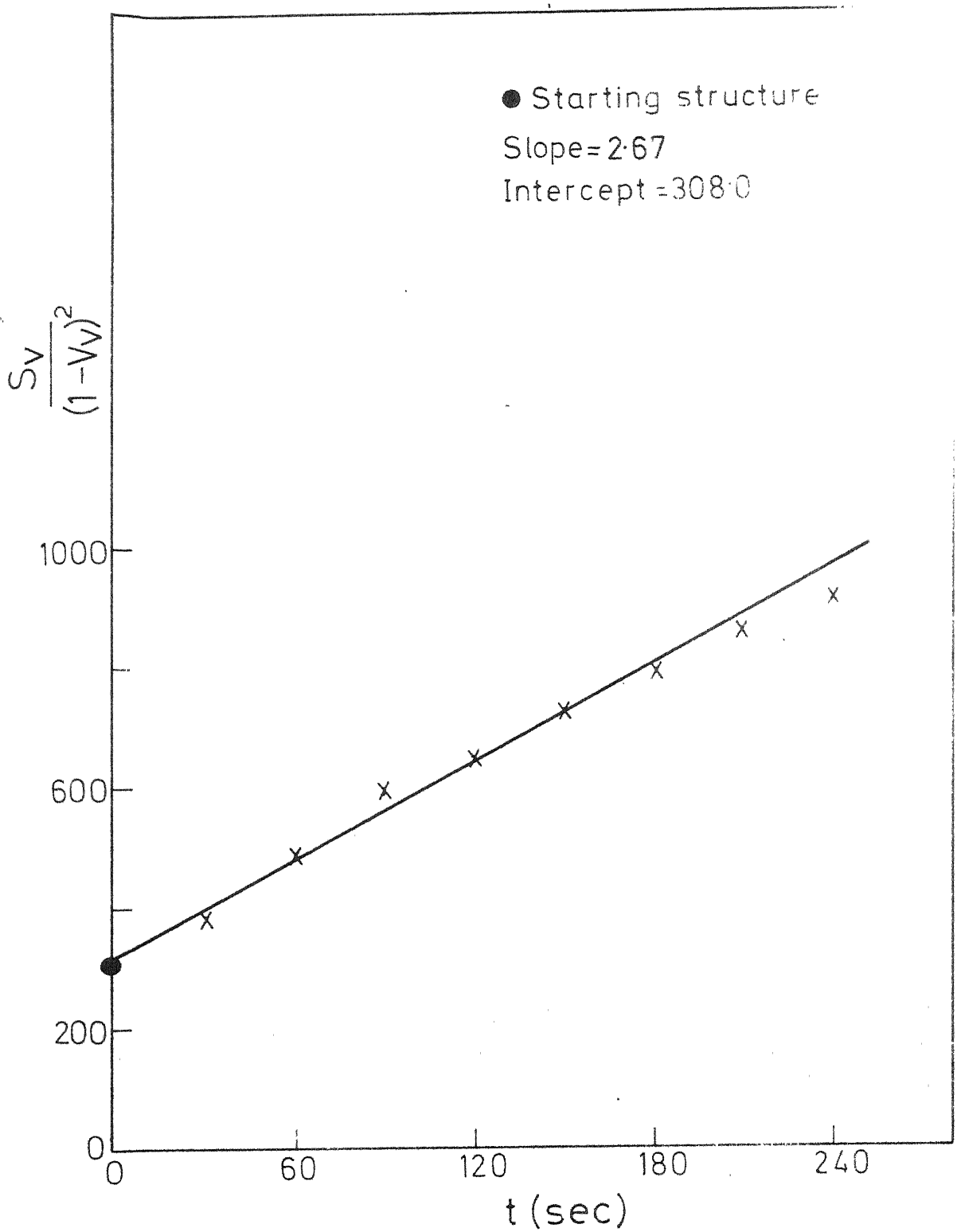

Fig.17 Plot of $\frac{S_V}{(1-V_V)^2}$ Vs t at 800 °C

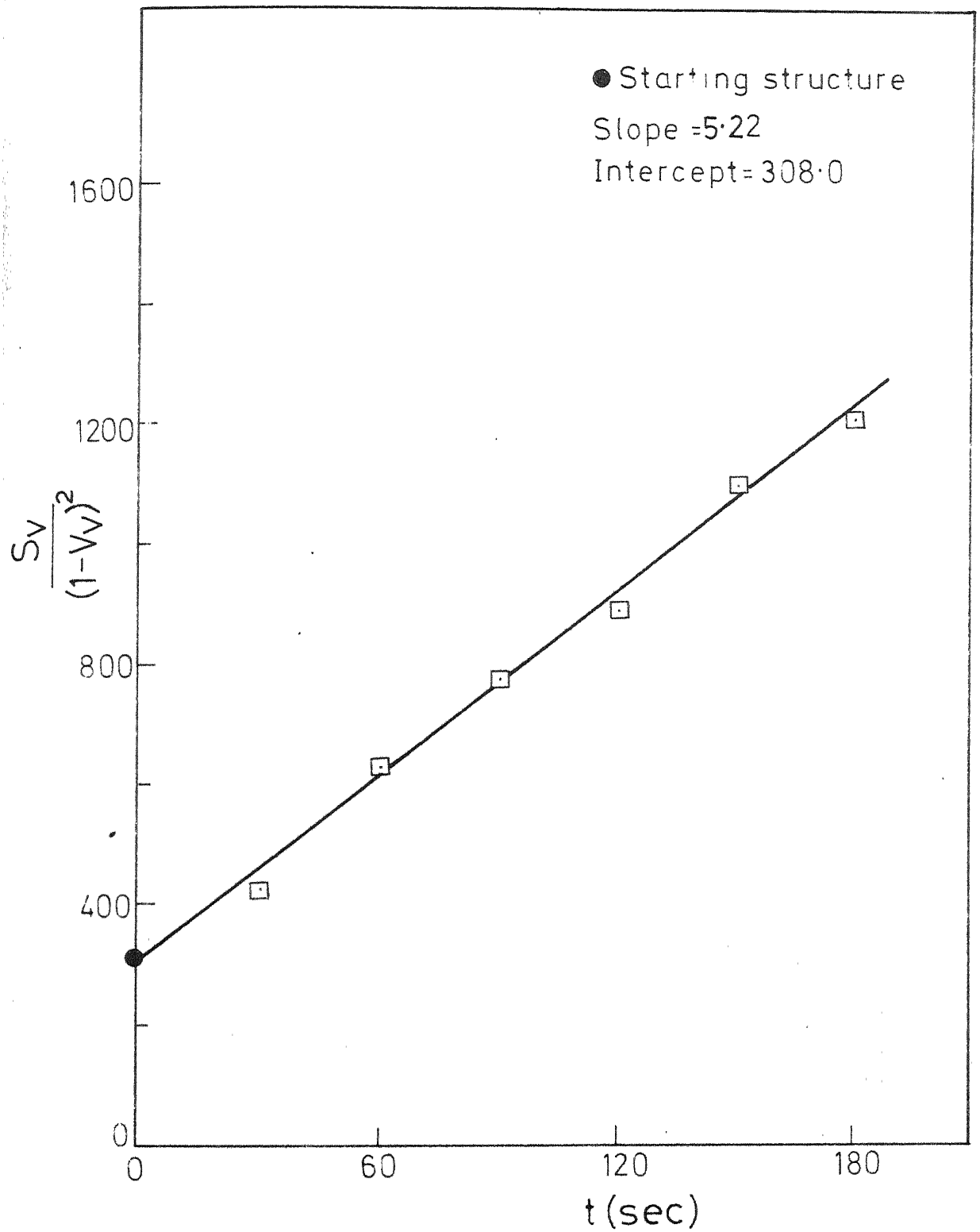

Fig.18 Plot of $\frac{S_V}{(1-V_V)^2}$ Vs t at 820 °C

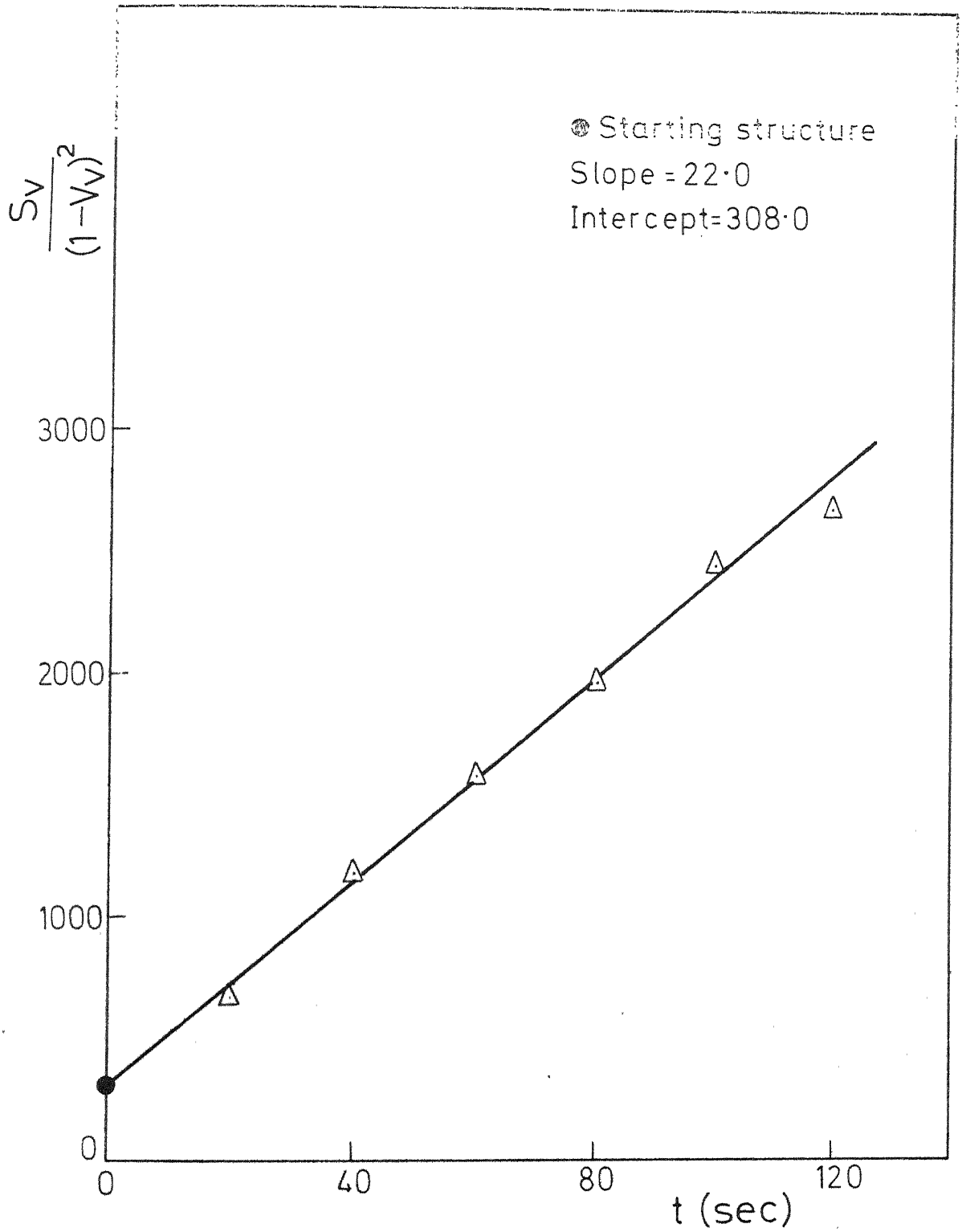

Fig.19 Plot of $\frac{S_V}{(1-V_V)^2}$ Vs t at 840 °C

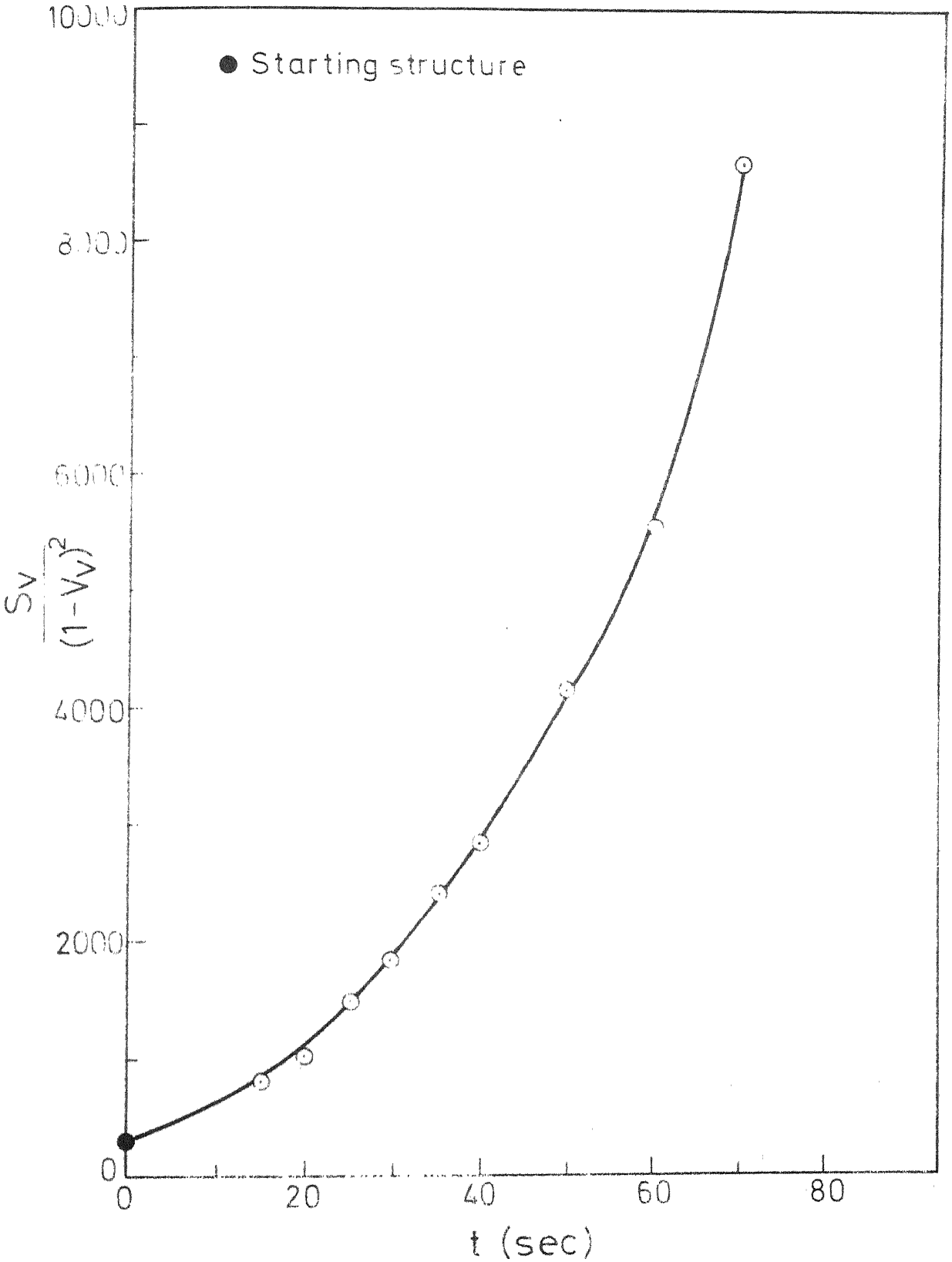

Fig.20 Plot of $\frac{S_V}{(1-V_V)^2}$ Vs t at 870 °C

where, E is the slope of the plot of $S_V/(1-V_V)^2$ vs. t, The values of E at 800°, 820° and 840°C are given in the Table - 8.

TABLE - 8

T°C	E cm^2/cm^3-sec
800	2.67
820	5.22
840	22.0

However, at 870°C the plot of $S_V/(1-V_V)^2$ vs. t is non linear (figure-20). A plot of $S_V/(1-V_V)^2$ vs. t^2 is found to be linear at 870°C (figure-21). Thus, at 870°C the time dependence of S_V can be described by the following equation

$$\frac{S_V}{(1-V_V)^2} = 309 + E_1 t^2 \qquad (5.7)$$

where, $E_1 = 1.66 \ cm^2/cm^3 - sec^2$

Thus, the time dependence of S_V at 870°C is different from that between 800° to 840°C. This again indicates that the rate controlling mechanism for austenite growth at 870°C is different from that between 800° to 840°C.

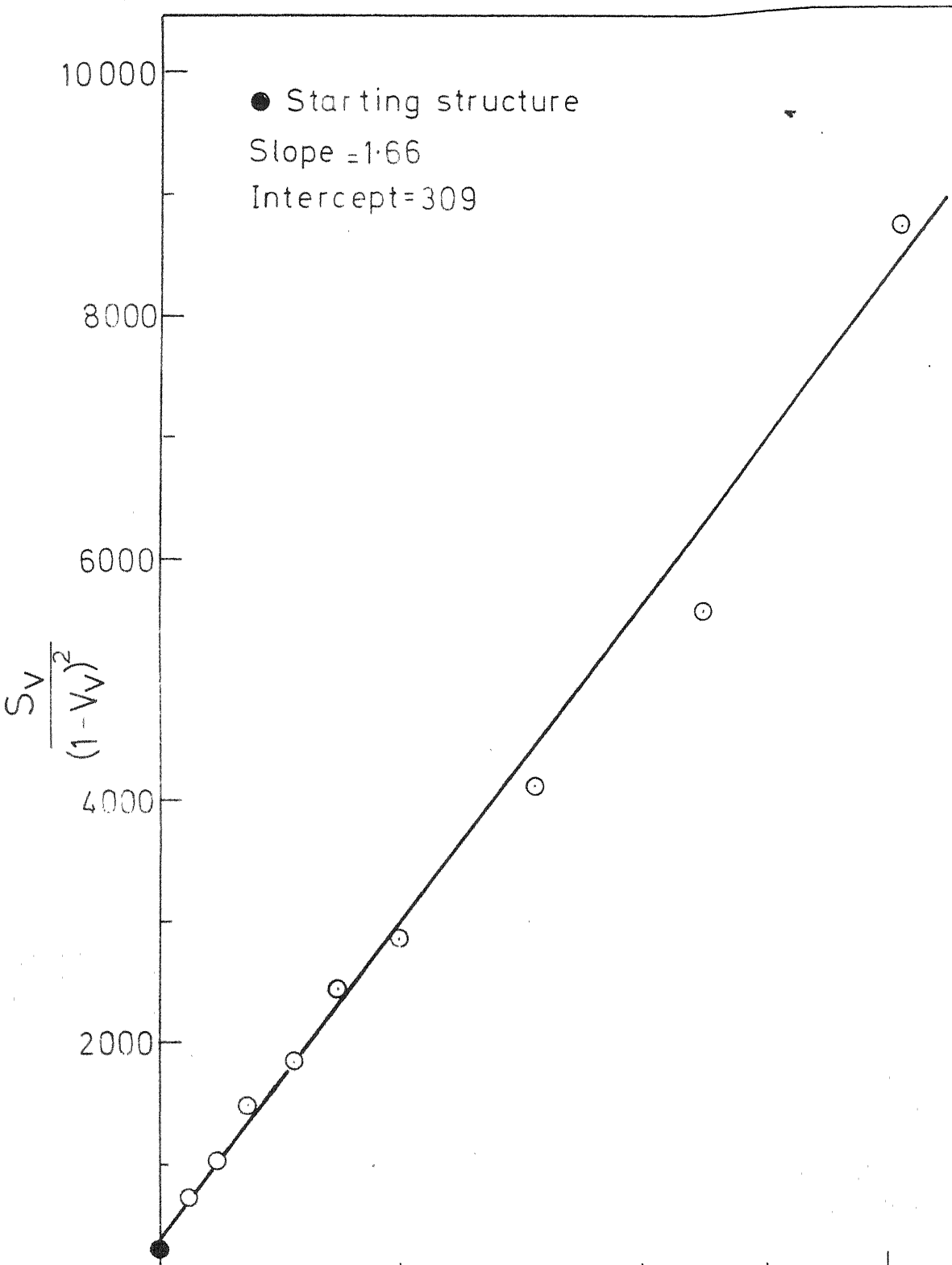

Fig.21 Plot of $\frac{S_V}{(1-V_V)^2}$ Vs t^2 at 870°C

5.4 Calculation of 'Extended' Volume Fraction and Surface Area :

In the starting microstructure, the pearlite nodules were mostly situated at the ferrite grain edges (triple points on the plane of polish). It follows that, the pearlite nodules are not randomly distributed in ferrite and so is true about the austenite particles. Thus, the geometrical impingement between the growing austenite particles can not be random. Hence, the impingement correction factors to obtain $S_{V_{ex}}$ and $V_{V_{ex}}$ from S_V and V_V can not be same as that for the random impingement. In this case since the product phase is clustered around the grain edges of ferrite, the impingement is clustered. In such a case the following impingement factors are applicable[17].

$$d\,V_V = (1-V_V)^2\, d\,V_{V_{ex}} \qquad (5.8)$$

$$\therefore \quad \frac{V_V}{1-V_V} = V_{V_{ex}} \qquad (5.9)$$

and

$$S_V = (1-V_V)^2\, S_{V_{ex}} \qquad (5.10)$$

or

$$\frac{S_V}{(1-V_V)^2} = S_{V_{ex}} \qquad (5.11)$$

In the recrystallization of Fe-Si alloys[18] and austenitization kinetics of spherodized cementite and ferrite aggregates[18] the product phase is situated at grain edges and the above impingement relations have been successfully used to interpret the kinetic data.

Combining equations (5.4) and (5.9) gives the following equation for the 'extended' volume fraction of austenite between 800° and 840°C

$$V_{V_{ex}} = B\ t + 0.19 \qquad (5.12)$$

Combining equations (5.9) and (5.5) gives the following relationship for the time dependence of $(V_V)_{ex}$ at 870°C

$$V_{V_{ex}} = B_1\ t^2 + 0.19 \qquad (5.13)$$

where, $B_1 = 0.00113$ per sec^2

Similarly, equations (5.6) and (5.11) lead to the following result for the time dependence of $S_{V_{ex}}$ between 800° and 840°C.

$$S_{V_{ex}} = E\ t + 308 \qquad (5.14)$$

whereas at 870°C we get

$$S_{V_{ex}} = E_1 t^2 + 309 \qquad (5.15)$$

where, $E_1 = 1.66\ cm^2/cm^3\text{-}sec^2$

Equation (5.3) can be written in the following form

$$\frac{S_V}{(1-V_V)^2} = K \frac{V_V}{1-V_V} \qquad (5.16)$$

Equations (5.9), (5.11) and (5.16) yield;

$$S_{V_{ex}} = K\ {}^{V}V_{ex} \qquad (5.17)$$

where, $K = 1446\ cm^2/cm^3$.

Note that equation (5.17) is valid at <u>all</u> the austenitization temperatures ranging from 800° to 870°C. This equation shows, that the extended surface area of the $\gamma - \alpha$ interface per unit volume $S_{V_{ex}}$ is <u>directly proportional</u> to the extended volume fraction of austenite and the relationship is valid at <u>all</u> the austenitizing temperatures studied. A correct interpretation of this result is extremely important for the further data analysis.

5.5 Growth Geometry for the Austenite Growth :

During the growth of the product phase, there are three possible growth geometrics,

(1) Shape preserving or three dimensional growth : During such a growth the quantitative particle shape does not change with time and hence for any given particle the growth rate is uniform in all the directions.

(2) Two dimensional growth : This involves radial growth of cylindrical particles whose length does not change with time. Thus the radii of the cylindrical product phase particles increase with time where as their length remain constant.

(3) One dimensional growth : This involves lengthening of rod shaped particles whose radii do not change with time.

Suppose that, austenite particles grow by a shape preserving or three dimensional growth. Let the variable R represent particle size. R will be a function of initial size ξ and process time t. The extended volume fraction and surface area are given by [19].

$$V_{V_{ex}} = K_V \int_0^{\xi_m} [R(\xi, t)]^3 \, n_V(\xi) \, d\xi \qquad (5.18)$$

$$S_{V_{ex}} = K_S \int_{c}^{\xi_m} [R(\xi, t)]^2 \, n_V(\xi) \, d\xi \qquad (5.19)$$

where, $n_V(\xi)$ is the initial size distribution function of the austenite particles and it is identical to the size distribution of the pearlite nodules. ξ_m is the size of largest pearlite nodule in the starting structure. K_V and K_S are the shape factors. $R(\xi, t)$ is the size of austenite particle at time t whose initial size was ξ. It is obvious that, for any non zero, non trivial functional form of $n_V(\xi)$ the integral on the R.H.S. of equation (5.18) can not be directly proportional to the integral on the R.H.S. of equation (5.19). It follows that $S_{V_{ex}}$ can not be directly proportional to $V_{V_{ex}}$ if the growth geometry is three dimensional. However, our experimental results indicate that $S_{V_{ex}}$ is directly proportional to $V_{V_{ex}}$ (equation 5.17). One may conclude that the austenite particles <u>do not</u> grow by a shape preserving three dimensional growth. Thus the growth geometry must be either two dimensional or one dimensional. An assumption of one dimensional growth would lead to a conclusion that the austenite growth rate increases with time at 870°C (this is demonstrated in appendix-1), which is impossible. One must conclude that the <u>austenite growth is two dimensional.</u>

Since the pearlite nodules are situated on the grain edges of ferrite, the austenite particles are also situated at the ferrite grain edge. In such a case, probable shape of the austenite particles is cylindrical. The cylinder axis is expected to be along the ferrite grain edge on which a given particle is situated. During a two dimensional growth of such austenite particles, the radius R increases with time where as the length $\bar{\Delta}$ remains constant. The length of the cylindrical particles, $\bar{\Delta}$ should be equal to the average ferrite grain edge length. For such a two dimensional growth, one can write;

$$V_{V_{ex}} = \pi \bar{\Delta} \int_{0}^{P_m} [R(P,t)]^2 n_V(p)dp \qquad (5.20)$$

where, R(p,t) is the radius of cylindrical austenite particle at time t whose initial radius is p, $n_V(P)$ is the initial size distribution of austenite which is the same as the distribution of pearlite nodules in ferrite. P_m is the radius of the largest pearlite nodule in the starting structure. $\bar{\Delta}$ is the length of cylindrical particles and it does not change with time.

The $S_{V_{ex}}$ is given by;

$$S_{V_{ex}} = 2\pi \int_0^{P_m} \left[R^2(P,t) + \bar{\Delta}\, R(P,t)\right] n_V(P)\, dp \qquad (5.21)$$

The second term in the square bracket (i.e. $\bar{\Delta}\ R(P,t)$) is expected to be much smaller as compared to the first term (i.e. $R^2(P,t)$) after some austenitization takes place. Thus;

$$S_{V_{ex}} = 2\pi \int_0^{P_m} \left[R(P,t)\right]^2 n_V(P)dp \qquad (5.22)$$

Combining equations (5.20) and (5.22) yields;

$$S_{V_{ex}} = \left(\frac{2}{\bar{\Delta}}\right).\ V_{V_{ex}} \qquad (5.23)$$

Equation (5.23) predicts a linear relationship between $S_{V_{ex}}$ and $V_{V_{ex}}$. Combining equations (5.9), (5.11) and (5.23) yields;

$$S_V = \frac{2}{\bar{\Delta}}\ V_V\ (1-V_V) \qquad (5.24)$$

where, $\bar{\Delta}$, the average ferrite grain edge length is independent of time and temperature of the austenitization process. This is precisely the experimentally observed relationship between S_V and V_V. Comparing equations (5.3) and (5.24) gives ;

$$\bar{\Delta} = 2/K = 14\mu \qquad (5.25)$$

From the above analysis one can conclude that the austenite growth geometry is two dimensional.

5.6 Estimation of Austenite Growth Rate :

Between 800°C to 840°C equation (5.12) gives the time dependence of $V_{V_{ex}}$.

$$V_{V_{ex}} = 0.19 + Bt \qquad (5.12)$$

Our model for two dimensional radial growth of cylinders gives;

$$V_{V_{ex}} = \pi\bar{\Delta}\int_0^{P_m} [R(P,t)]^2 \, n_V(P)dp \qquad (5.20)$$

Combining equations (5.12) and (5.20) yields,

$$\pi\bar{\Delta}\int_0^{P_m} [R(P,t)]^2 \, n_V(P)dp = 0.19 + Bt \qquad \ldots\ldots (5.26)$$

Operating on equation (5.26) by d/dt gives,

$$\frac{B}{\pi\bar{\Delta}} = \int_0^{P_m} \left(\frac{\partial R^2}{\partial t}\right)_p n_V(P)\, dp \qquad (5.27)$$

L.H.S. of the equation is independent of time and it depends only on the temperature. The integral on the R.H.S. of equation (5.27) can be independent of time if and only if $(\frac{\partial R^2}{\partial t})_p$ is constant at a given temperature. One can conclude that

$$(\frac{\partial R^2}{\partial t})_p = \alpha^2(T) \qquad (5.28)$$

where, $\alpha^2(T)$ is a function of temperature only. Combining equations (5.27) and (5.28) yields;

$$\frac{B}{\pi \bar{\Delta}} = \alpha^2(T) \int_0^{P_m} n_V(P)dp = \alpha^2(T) \cdot N_V \qquad (5.29)$$

or

$$\alpha^2(T) = \frac{B}{\pi \bar{\Delta} N_V} \qquad (5.30)$$

where, N_V is the total number of pearlite nodules per unit volume in the initial structure. This is identically equal to the 'extended' number of austenite particles per unit volume at any time during the second stage of the austenitization process, because there is no further nucleation of austenite during the second stage of the austenitization process. The parameter N_V is independent of the time and temperature of the austenitization process and it is completely determined by the starting microstructure.

The equations (5.28) and (5.30) yields;

$$\left(\frac{\partial R^2}{\partial t}\right)_p = \alpha^2(T) = \frac{B}{\pi \bar{\Delta} N_V} \qquad (5.31)$$

Note that equation (5.31) is valid for any arbitrary initial size distribution of the pearlite nodules. The integration of equation (5.31) gives the following result for the growth paths of the austenite particles.

$$R^2 = P^2 + \alpha^2(T)\, t \qquad (5.32)$$

Thus one can conclude that between 800°C & 840°C, the austenitization process takes place by a radial <u>parabolic</u> growth of the cylindrical austenite particles. This growth law indicates a <u>diffusion controlled</u> growth of austenite between 800°C and 840°C.

Combining equations (5.20) and (5.13) gives the following result for the austenitization process at 870°C.

$$0.19 + B_1 t^2 = \pi \bar{\Delta} \int_0^{P_m} [R(P,t)]^2 n_V(P) dP \qquad (5.33)$$

Operating on the above equation by d^2/dt^2 gives;

$$B_1 = \pi \bar{\Delta} \int_0^{P_m} \left(\frac{\partial^2 R^2}{\partial t^2}\right)_P n_V(P)\, dP \qquad (5.34)$$

The above equation is valid at any austenitization time. The integral on the right hand side of this equation can be independent of time if and only if $(\partial^2 R^2/\partial t^2)_P$ is a constant at a given temperature. Thus, one can conclude that, for the austenitization process at 870°C;

$$(\frac{\partial^2 R^2}{\partial t^2})_P = \text{constant} = \beta(T) \qquad (5.35)$$

and $$\beta(T) = B_1/\pi \quad N_V \qquad (5.36)$$

Note that equations (5.35) and (5.36) are valid for any arbitrary initial size distribution of pearlite nodules. The growth behaviour described by equation (5.30) can be explained if the radial growth rate of the austenite particles is <u>constant</u> at a given temperature. This can be demonstrated as follows.

Let; Radial growth rate $= (\frac{\partial R}{\partial t})_P = \text{constant}$

$$= \frac{\beta(T)}{2}^{\frac{1}{2}} \qquad (5.37)$$

Thus; $$R = P + \left[\frac{\beta(T)}{2}\right]^{\frac{1}{2}} t \qquad (5.38)$$

Now, $$(\frac{\partial R^2}{\partial t})_P = 2R\,(\frac{\partial R}{\partial t})_P \qquad (5.39)$$

Hence, $\left(\frac{\partial R^2}{\partial t}\right)_P = 2\left[\frac{\beta(T)}{2}\right]^{\frac{1}{2}}\left\{P + \left[\frac{\beta(T)}{2}\right]^{\frac{1}{2}} t\right\}$ (5.40)

Operating on equation (5.40) by $\left(\partial/\partial t\right)_P$ yields;

$$\left(\frac{\partial^2 R^2}{\partial t^2}\right)_P = \beta(T) \qquad (5.35)$$

From the above analysis one can conclude that at 870°C the radial growth rate of austenite particles is constant. This indicates that at 870°C the austenitization process probably occurs by a massive transformation or interface controlled growth.

5.7 Estimation of Growth Parameters :

For the austenitization process between 800°C and 840°C, the parabolic growth rate constant $\alpha^2(T)$ can be estimated at various temperatures by utilizing equation (5.31).

$$\alpha^2(T) = \frac{B}{\pi \bar{\Delta} N_V} \qquad (5.31)$$

Values of B (Table-7) and $\bar{\Delta}$ ($=14\times10^{-4}$ cm) are known. Thus, $\alpha^2(T)$ can be calculated if N_V is known.

An approximate calculation of the number of pearlite nodules per unit volume N_V can be carried out as follows.

Assume that all the pearlite nodules have the same radius P_o and length $\bar{\Delta}$. The initial volume fraction of pearlite is 0.16. Thus;

$$0.16 = \pi \bar{\Delta} \; P_o^2 \; N_V \qquad (5.41)$$

It can be shown that the number of pearlite patches per unit area of the plane of polish N_A is given by[20]

$$N_A = N_V \bar{D} \qquad (5.42)$$

where, $\bar{D}$ is the mean calipre diameter[20] of the particles. For the cylindrical particles Dehoff[21] has shown that the mean calipre diameter is given by ;

$$\bar{D} = \frac{\pi P_o + \bar{\Delta}}{2} \qquad (5.43)$$

Combining equations (5.42) and (5.43) yields;

$$N_A = \frac{N_V}{2} \left(\pi \; P_o + \bar{\Delta} \right) \qquad (5.44)$$

The quantity N_A can be measured on the plane of polish. For the initial microstructure it was observed that;

$$N_A = 2.1 \times 10^4 \text{ per cm}^2$$

Thus,

$$2.1 \times 10^4 = \frac{N_V}{2} \left(\pi \; P_o + \bar{\Delta} \right) \qquad (5.45)$$

Since, $\bar{\Delta}$ is already known, the solution of the simultaneous equations (5.41) and (5.45) gives the following values of P_o and N_V

$$\begin{aligned} N_V &= 6.4 \times 10^{6} \text{ per cm}^3 \\ P_o &= 2.5 \times 10^{-3} \text{ cm} \\ \bar{\Delta} &= 14 \times 10^{-4} \text{ cm} \end{aligned} \qquad (5.46)$$

Using the above values of $\bar{\Delta}$ and N_V and values of B from Table - 7, the $\alpha^2(T)$ can be calculated by utilizing equation (5.31). The values of $\alpha^2(T)$ calculated in this manner are given in Table - 9.

TABLE - 9

T°C	α^2 (T) $cm^2/sec.$
800	5.8×10^{-8}
820	12.8×10^{-8}
840	53.3×10^{-8}

At 870°C the constant growth rate parameter is $(\frac{\beta(T)}{2})^{\frac{1}{2}}$ (see equation 5.37). Since B_1, $\bar{\Delta}$ and N_V in equation (5.36) are known, the $\beta(T)$ can be calculated, Thus,

Constant growth rate parameter at 870°C = $(\frac{\beta(T)}{2})^{\frac{1}{2}}$

$= 14.2 \times 10^{-8}$ cm/sec.

CHAPTER VI

CONCLUSIONS

(1) During the austenitization kinetics of Fe-0.15%C alloy (whose starting microstructure consists of pearlite nodules distributed in ferrite matrix), the volume fraction of austenite V_V is related to the corresponding value of the surface area of the austenite-ferrite interface per unit volume S_V by the following equation.

$$S_V = K\ V_V\ (1-V_V)$$

The parameter K is independent of temperature and process time. It is completely determined by the starting microstructure. In the present case, K is equal to 1446 cm^2/cm^3.

(2) Between 800°C to 840°C the time dependence of the volume fraction of austenite can be described by the following equation

$$\frac{V_V}{1-V_V} = B\ t + 0.19$$

The parameter B depends on the austenitization temperature. However, at 870°C the volume fraction of

austenite varies with time in the following manner.

$$\frac{V_V}{1 - V_V} = B_1 t^2 + 0.19$$

(3) Between 800°C to 840°C, the time dependence of the austenite-ferrite surface area per unit volume S_V can be described by;

$$\frac{S_V}{(1-V_V)^2} = 308 + E\ t$$

The parameter E depends on austenitizing temperature and it is independent of the process time. However, at 870°C the relationship between S_V, V_V and t is given by;

$$\frac{S_V}{(1-V_V)^2} = E_1 t^2 + 309$$

(4) The austenite particles are clustered around the ferrite grain edges. Thus, the geometrical impingement between the growing austenite particles is not random. The extended global properties are related to their corresponding real values by the following equations.

$$V_{V_{ex}} = \frac{V_V}{(1-V_V)}$$

$$S_{V_{ex}} = \frac{S_V}{(1-V_V)^2}$$

(5) The extended surface area of the $\gamma - \alpha$ interface per unit volume $S_{V_{ex}}$ is directly proportional to the extended volume fraction of austenite $V_{V_{ex}}$. The proportionality constant is independent of temperature and process time.

(6) The growth geometry of austenite particles is two dimensional. The austenite particles have a cylindrical shape. Their radius increases with time but the length remains constant.

(7) Between 800°C to 840°C, the second stage of the austenitization process occurs by a two dimensional radial parabolic growth of the austenite particles. The radius R of the cylindrical particles increases with time in the following manner.

$$R^2 = P^2 + \alpha^2 (T). t$$

where, P is the initial cylinder radius of austenite particle which has radius R at time t. $\alpha^2(T)$ is the parabolic growth rate constant and it depends on temperature. The value of $\alpha^2(T)$ has been estimated at 800°C, 820°C and 840°C. (see Table - 9).

(8) Between 800°C to 840°C, the austenite growth is diffusion controlled.

(9) At 870°C, the radial growth rate of austenite particles is constant. This probably indicates that the austenite growth is interface controlled or the process occurs by massive transformation. However, this conclusion is only tentative. More experimental work at temperatures higher than 870°C is necessary before arriving at a definite conclusion.

(10) By proper choice of the system, the nucleation rate variable is eliminated. Using this strategy, growth rate of austenite has been deduced between 800°C to 870°C from the experimental data.

APPENDIX I

One dimensional growth geometry involves lengthening of rod like particles whose cross sectional area remains constant. Let $\bar{A}$ be the area of cross section of the rod like particles and let the variable L represent the rod lengths. The length L of a given particle depends on its initial length λ and the process time t. The extended volume fraction of austenite is given by;

$$V_{V_{ex}} = \bar{A} \int_0^{\lambda_m} L(\lambda, t)\, n_V(\lambda)\, d\lambda \qquad (1\text{-A})$$

where, $n_V(\lambda)$ is the initial size distribution of the rod lengths in the starting structure and λ_m is the length of the longest rod in the starting structure. Combining equations (1-A) and (5.5) yields;

$$0.19 + B_1 t^2 = \bar{A} \int_0^{\lambda_m} L(\lambda, t) n_V(\lambda)\, d\lambda \qquad (2\text{-A})$$

Operating on equation (2-A) by d^2/dt^2 gives;

$$2B_1 = \bar{A} \int_0^{\lambda_m} \left(\frac{\partial^2 L}{\partial t^2}\right)_\lambda n_V(\lambda)\, d\lambda \qquad (3\text{-A})$$

The L.H.S. of equation (3-A) is independent of time. Thus the integral on the R.H.S. of equation (3-A) must be time independent. This is possible if and only if

$$\left(\frac{\partial^2 L}{\partial t^2}\right)_\lambda = \text{constant} = \gamma'(T) \qquad (4\text{-A})$$

Integration of this equation yields,

$$\text{Lengthening growth rate} = \left(\frac{\partial L}{\partial t}\right)_\lambda = \gamma'(T)t + F \qquad (5\text{-A})$$

where, F is the constant of integration. Equation (5-A) indicates that the lengthening growth rate $(\partial L/\partial t)_\lambda$ <u>increases</u> with time. This is impossible, because growth rate of any real process either decreases with time or remains constant. We must conclude that the austenite growth geometry can not be one dimensional.

REFERENCES

1. W.A. Jhonson and R.F. Mehl., Trans. AIME, 1939, Vol. 135, P. 416.
2. R.T. DeHoff, "The Dynamics of Microstructural Change" in Treatise on Materials Science and Technology, 1972, Vol. 1, P. 247.
3. G.R. Speich and A. Szirmae, J.I. S.I., 1968, Vol.206, P. 385.
4. G.A. Roberts and R.F. Mehl, Trans. AIME, 1943, Vol. 31, P. 613.
5. R.R. Judd and H.W. Paxton, Trans. AIME, 1968, Vol. 242, P. 206-214.
6. G.R. Speich and A. Szirmae, Trans. AIME, Vol. 245, P. 1063.
7. S. Niedzweidz, B. Weiss and Y-Partom, ASM, Trans. Quart., 1964, Vol. 62, P. 11-17.
8. B. Karlson, Z. Metallik., 1972, Vol. 63, P. 160.
9. A. Delesse, Ann. Mines IV, 1848, Vol. 13, P. 379.
10. A. Rosiwal, K.K. Geol. Reich. Wien, 1898, Vol. 6, P. 143.
11. E. Thomson, J. Geol., 1930, Vol. 38, P. 193.
12. A.A. Glagolev., Eng. Min. J., 1934, Vol. 135, P.399.

13. J.E. Hilliard and J.W. Cahn, Trans. AIME, 1961, Vol. 221, P. 344.

14. S.A. Saltykov, Stereometric Metallography, 2nd ed., Metallurgizdat, Moscow, 1958.

15. C.S. Smith and L. Guttman, Trans. AIME, 1953. Vol. 197, P. 81.

16. W.A. Jhonson and R.F. Mehl, Trans. AIME, 1939, Vol.135, P. 416.

17. R.T. DeHoff, "The Dynamics of Microstructural Change," Treatise on Materials Science and Tech.,' 1972, Vol. 1, P. 247.

18. A.M. Gokhale, Ph.D. Thesis, University of Florida, March, 1977.

19. A.M. Gokhale and R.T. DeHoff, To Be Published.

20. R.T. DeHoff and F.N. Rhines, Quantitative Microscopy, McGraw-Hill, New York, 1968.

21. R.T. DeHoff, Met. Trans. A, in Press.

LIST OF CORRECTIONS

	Page No.
Read "Spheroidized" instead of "spherodised"	6,7,8,9
Read "Karlsson" instead of "Karlson"	9, 10, 11
Exclude "the" in the second line from bottom	9
Read "Problem" instead of "pronblem" in the eleventh line from top	10
Read "Karlsson's data" instead of "Kartson's data"	12
Exclude 'δ' from equation (5.9)	52